Cellular evidence on how nicotine and e-cigarettes increase cancer risk in humans (and mice)

January 30, 2018

Stanton A. Glantz, PhD

It is an article of faith at the FDA and among e-cigarette enthusiasts that nicotine is not carcinogenic and that e-cigarettes do not pose any substantial cancer risk because the levels of carcinogens in e-cigarette aerosol is much lower than in a conventional cigarette.

These beliefs are challenged by a recent paper, "E-cigarette smoke damages DNA and reduces repair

activity in mouse lung, heart, and bladder as well as in human lung and bladder cells," by Hyun-Wook Lee and colleagues at NYU. They exposed live mice to light levels of e-cigarette aerosol and found damage to the DNA in lung, heart and bladder cells as well as in human lung and bladder cells. They found that the cells themselves converted nicotine to carcinogenic NNN and NNK even if it was not in the original e-cigarette aerosol. They also found that exposure to nicotine and e-cigarette aerosol damaged normal DNA repair

Stanton A. Glantz, PhD
Director, Center for Tobacco Research Control & Education

Latest Blog Articles

mechanisms.

Here is how they sum up the significance of their findings:

> E-cigarette smoke (ECS) delivers nicotine through aerosols without burning tobacco. ECS is promoted as noncarcinogenic. We found that ECS induces DNA damage in mouse lung, bladder, and heart and reduces DNA-repair functions and proteins in lung. Nicotine and its nitrosation product 4-(methylnitrosamine)-1-(3-pyridyl)-1-butanone can cause the same effects as ECS and enhance mutations and tumorigenic cell transformation in cultured human lung and bladder cells. These results indicate that nicotine nitrosation occurs in the lung, bladder, and heart, and that its products are further metabolized into DNA damaging agents. We propose that ECS, through damaging DNA and inhibiting DNA repair, might contribute to human lung and bladder cancer as well as to heart disease, although further studies are required to substantiate this proposal.

This paper is particularly important because it is identifying direct molecular mechanisms by which this damage occurs.

This study also directly starts to fill the data gap identified in the recent National Academies of Science, Engineering, and Medicine report on e-cigarettes, which states, "There is no available evidence whether or not e-cigarette use is associated with intermediate cancer endpoints in humans." This new paper demonstrates such an association at the subcellular level.

It's too bad that the paper did not include a comparison group exposed to cigarette smoke, but these results nevertheless indicate that the FDA (and others) need to stop being so glib

Cellular evidence on how nicotine and e-cigarettes increase cancer risk in humans (and mice)

TV show hyped Philip Morris' latest tobacco product

IQOS is expanding the nicotine addiction market in Italy

Recreational marijuana legalization followed by drop in opioid deaths in Colorado

Kids who smoke even one day a month are more likely to smoke as young adults

in making statements that nicotine doesn't have any cancer effects.

Here is the abstract:

> E-cigarette smoke delivers stimulant nicotine as aerosol without tobacco or the burning process. It contains neither carcinogenic incomplete combustion byproducts nor tobacco nitrosamines, the nicotine nitrosation products. E-cigarettes are promoted as safe and have gained significant popularity. In this study, instead of detecting nitrosamines, we directly measured DNA damage induced by nitrosamines in different organs of E-cigarette smoke exposed mice. We found mutagenic O6-methyldeoxyguanosines and γ-hydroxy-1,N2-propano-deoxyguanosines in the lung, bladder, and heart. DNA-repair activity and repair proteins XPC and OGG1/2 are significantly reduced in the lung. We found that nicotine and its metabolite, nicotine-derived nitrosamine ketone, can induce the same effects and enhance mutational susceptibility and tumorigenic transformation of cultured human bronchial epithelial and urothelial cells. These results indicate that nicotine nitrosation occurs in vivo in mice and that E-cigarette smoke is carcinogenic to the murine lung and bladder and harmful to the murine heart. It is therefore possible that E-cigarette smoke may contribute to lung and bladder cancer, as well as heart disease, in humans.

Needless to say, the pro-industry Science Media Center is already poo-point the study.

The full citation is: Hyun-Wook Lee, Sung-Hyun Park, Mao-wen Weng, Hsiang-Tsui Wang, William C. Huang, Herbert Lepor, Xue-Ru Wu, Lung-Chi Chen and Moon-shong Tang. E-cigarette smoke damages DNA and reduces repair activity in mouse lung, heart, and

repair activity in mouse lung, heart, and bladder as well as in human lung and bladder cells. PNAS 2018; published ahead of print January 29, 2018, https://doi.org/10.1073/pnas.1718185115. It is available here.

Add new comment

Your name

Comment *

Preview

E-cigarette smoke damages DNA and reduces repair activity in mouse lung, heart, and bladder as well as in human lung and bladder cells

Hyun-Wook Lee[a,1], Sung-Hyun Park[a,1], Mao-wen Weng[a,1], Hsiang-Tsui Wang[a], William C. Huang[b], Herbert Lepor[b], Xue-Ru Wu[b], Lung-Chi Chen[a], and Moon-shong Tang[a,2]

[a]Department of Environmental Medicine, New York University School of Medicine, Tuxedo Park, NY 10987; and [b]Department of Urology, New York University School of Medicine, New York, NY 10016

Edited by Bert Vogelstein, Johns Hopkins University, Baltimore, MD, and approved December 20, 2017 (received for review October 17, 2017)

E-cigarette smoke delivers stimulant nicotine as aerosol without tobacco or the burning process. It contains neither carcinogenic incomplete combustion byproducts nor tobacco nitrosamines, the nicotine nitrosation products. E-cigarettes are promoted as safe and have gained significant popularity. In this study, instead of detecting nitrosamines, we directly measured DNA damage induced by nitrosamines in different organs of E-cigarette smoke-exposed mice. We found mutagenic O^6-methyldeoxyguanosines and γ-hydroxy-1,N^2-propano-deoxyguanosines in the lung, bladder, and heart. DNA-repair activity and repair proteins XPC and OGG1/2 are significantly reduced in the lung. We found that nicotine and its metabolite, nicotine-derived nitrosamine ketone, can induce the same effects and enhance mutational susceptibility and tumorigenic transformation of cultured human bronchial epithelial and urothelial cells. These results indicate that nicotine nitrosation occurs in vivo in mice and that E-cigarette smoke is carcinogenic to the murine lung and bladder and harmful to the murine heart. It is therefore possible that E-cigarette smoke may contribute to lung and bladder cancer, as well as heart disease, in humans.

E-cigarettes | DNA damage | DNA repair | lung–bladder–heart | cancer

E-cigarettes (E-cigs) are designed to deliver the stimulant nicotine, similar to conventional cigarettes, through an aerosol state. In E-cigs, nicotine is dissolved in relatively harmless organic solvents, such as glycerol and propylene glycol, then aerosolized with the solvents by controlled electric heating. Hence, E-cig smoke (ECS) contains mostly nicotine and the gas phase of the solvents (1–4). In contrast, conventional tobacco smoke (TS), in addition to nicotine and its nitrosamine derivatives, contains numerous (>7,000) incomplete combustion byproducts, such as polycyclic aromatic hydrocarbons (PAHs), aromatic amines, aldehydes, and benzene, many of which are human carcinogens, irritants, and allergens (5, 6). TS also has a strong scent. Therefore, TS is both harmful and carcinogenic to smokers, as well as being unpleasant and harmful to bystanders (7). Because of these effects, TS has become an unwelcome social habit and is no longer acceptable in many social settings and public domains (8). E-cigs have been promoted as an alternative to cigarettes that can deliver a TS "high" without TS's ill and unpleasant effects. Since it appears that ECS contains neither carcinogens, allergens, nor odors that result from incomplete combustion, as a result of these claims, E-cigs have become increasingly popular, particularly with young people (9). However, the question as to whether ECS is as harmful as TS, particularly with regard to carcinogenicity, remains a serious public health issue that deserves careful examination.

It is well established that most chemical carcinogens, either directly or via metabolic activation, can induce damage in genomic DNA, that unrepaired DNA damage can induce mutations, and that multiple mutations can lead to cancer (10). Many chemical carcinogens can also impair DNA-repair activity (11–13). Therefore, in this study, as a step to understanding the carcinogenicity of ECS, we determined whether ECS can induce DNA damage in different organs of a mouse model and whether ECS can affect DNA-repair activity. We then characterized the chemical nature of ECS-induced DNA damage and how ECS affects DNA repair. Last, we determined the effect of ECS metabolites on the susceptibility to mutations and tumorigenic transformation of cultured human cells.

Results

ECS Induces O^6-Methyl-Deoxuguanosine in the Lung, Bladder, and Heart. Nicotine is the major component of ECS (3). The majority (80%) of inhaled nicotine in smoke is quickly metabolized into cotinine, which is excreted into the bloodstream and subsequently into urine (14). Cotinine is generally believed to be nontoxic and noncarcinogenic (15); however, a small portion (<10%) of inhaled nicotine is believed to be metabolized into nitrosamines in vivo (16–18). Nitrosamines induce tumors in different organs in animal models (6, 19). Inhaled nitrosamines are metabolized into *N*-nitrosonornicotine (NNN) and nicotine-derived nitrosamine ketone (NNK). It has been proposed that NNK can be further metabolized and spontaneously degraded

Significance

E-cigarette smoke (ECS) delivers nicotine through aerosols without burning tobacco. ECS is promoted as noncarcinogenic. We found that ECS induces DNA damage in mouse lung, bladder, and heart and reduces DNA-repair functions and proteins in lung. Nicotine and its nitrosation product 4-(methylnitrosamine)-1-(3-pyridyl)-1-butanone can cause the same effects as ECS and enhance mutations and tumorigenic cell transformation in cultured human lung and bladder cells. These results indicate that nicotine nitrosation occurs in the lung, bladder, and heart, and that its products are further metabolized into DNA damaging agents. We propose that ECS, through damaging DNA and inhibiting DNA repair, might contribute to human lung and bladder cancer as well as to heart disease, although further studies are required to substantiate this proposal.

Author contributions: H.-W.L., S.-H.P., M.-w.W., H.-T.W., L.-C.C., and M.-s.T. designed research; H.-W.L., S.-H.P., M.-w.W., H.-T.W., and M.-s.T. performed research; M.-s.T. contributed new reagents/analytic tools; H.-W.L., S.-H.P., M.-w.W., W.C.H., H.L., X.-R.W., and M.-s.T. analyzed data; and H.-W.L., S.-H.P., M.-w.W., H.-T.W., W.C.H., H.L., X.-R.W., L.-C.C., and M.-s.T. wrote the paper.

The authors declare no conflict of interest.

This article is a PNAS Direct Submission.

[1]H.-W. L., S.-H. P., and M.-w.W. contributed equally to this work.

[2]To whom correspondence should be addressed. Email: moon-shong.tang@nyumc.org.

This article contains supporting information online at www.pnas.org/lookup/suppl/doi:10.1073/pnas.1718185115/-/DCSupplemental.

into methyldiazohydroxide (MDOH), pyridyl-butyl derivatives (PBDs), and formaldehyde, and that NNN degrade into hydroxyl or keto PBDs (20). While nicotine cannot bind to DNA directly, MDOH can methylate deoxyguanosines and thymidines in DNA (21). Although the fate of nitrosamine-induced formaldehyde and PBDs in vivo is less clear, both are capable of inducing DNA damage in vitro (22–25). Therefore, if ECS in fact is a carcinogen, it is likely that its carcinogenicity is derived from nitrosamines that are derived from the nitrosation of nicotine (5, 19, 21). Nitrosamines are potent carcinogens and it is generally believed that their carcinogenicity is via induction of methylation DNA damage (26, 27). As a step in examining the carcinogenicity of ECS, we determined whether ECS can induce O^6-methyl-deoxuguanosine (O^6-medG) adducts in lung, heart, liver, and bladder tissues of mice. Mice were exposed to ECS (10 mg/mL, 3 h/d, 5 d/wk) for 12 wk; the dose and duration equivalent in human terms to light E-cig smoking for 10 y. The results in Fig. 1 *A* and *B*, Fig. S1, and Table S1 show that ECS induced significant amounts of O^6-medG adducts in the lung, bladder, and heart and that the level of O^6-medG adducts in lung was three- to eightfold higher than in the bladder and heart. These results are consistent with the explanation that nicotine is metabolized into MDOH, which can methylate DNA (16, 20).

ECS Induces γ-OH-PdG in the Lung, Bladder, and Heart. Recently, we found that aldehyde-derived cyclic 1,N^2-propano-dG (PdG), including γ-OH-1,N^2-PdG (γ-OH-PdG) and α-methyl-γ-OH-1,N^2-PdG adducts, are the major DNA adducts in mouse models (28) induced by TS, which contains abundant nitrosamines and aldehydes (20). We therefore determined the extent of PdG formation in different organs of ECS-exposed mice using a PdG-specific antibody (28–30).

The results in Fig. 1 *C* and *D* show that ECS induced PdG adducts in the lung, bladder, and heart, and that the level of PdG in the lung is two- to threefold higher than in the bladder and heart. Moreover, the level of PdG is 25- to 60-fold higher than the level of O^6-medG in lung, bladder, and heart tissues, indicating that induction of PdG is more efficient than induction of O^6-medG by nicotine metabolic products and/or that O^6-medG is more efficiently repaired in these organs. ECS, however, did not induce either O^6-medG or PdG in liver DNA.

Due to the relatively minute amount of genomic DNA that is possible to isolate from mouse organs, in this case, specifically from bladder mucosa, which is only able to yield up to 2 μg of genomic DNA from each mouse, we used the sensitive ^{32}P-postlabeling thin layer chromatography (TLC)/HPLC method to identify the species of the PdG formed in lung and bladder tissues (13, 28, 31). The results in Fig. 1*E* show that the majority of PdG (>95%) formed in these tissues coelute with γ-OH-PdG adduct standards with a minor portion that coelute with α-OH-PdG standards.

Relationship of ECS-Induced PdG and O^6-medG Formation in Different Organs of Each Animal. We then determined the relationship of PdG and O^6-medG formation in different organs of each animal. The results in Fig. 2*A* show that the levels of PdG and O^6-medG in the same organs are positively related to each other. Thus, a lung tissue sample that had a high level of PdG also had a high level of O^6-medG. The same relationship between PdG and O^6-medG formation was found in the bladder and heart (Fig. 2*A* and Table S1). The results in Fig. 2*B* show that in the same mouse, the levels of PdG and O^6-medG formation in different organs also have a positive correlation: Mice with a high level of PdG and O^6-medG formation in the lung also had a high level of these DNA adducts in the bladder and heart (Fig. 2*B* and Table S1). Together, these results indicate that the formation of PdG and O^6-medG DNA adducts in the lung, bladder, and heart tissue are the result of DNA damaging agents derived from ECS exposure, and raising the possibility that the ability for nicotine absorption and metabolism and DNA-repair activity of different organs determine their susceptibility to ECS-induced DNA adduct formation.

ECS Reduces DNA-Repair Activity in the Lung. Recently, we have found that lung tissues of mice exposed to TS have lower DNA-repair activity and lower levels of DNA-repair proteins XPC and OGG1/2 and that aldehydes, such as acrolein, acetaldehyde, crotonaldehyde, and 4-hydroxy-2-nonenal, can modify DNA-repair proteins, causing the degradation of these repair proteins and impairing DNA-repair function (11, 12, 28). These findings raise the possibility that, via induction of aldehydes, ECS can impair DNA-repair functions. To test this possibility, we determined the effect of ECS on the activity of the two major DNA-repair mechanisms in mouse lung tissues: nucleotide excision repair (NER) and base excision repair (BER) (32). We adopted a well-established in vitro DNA damage-dependent repair synthesis assay, which requires only 10 μg of freshly prepared cell lysates (11, 13, 28). Since the amount of bladder mucosa collected from individual mice was minute, we were only able to determine DNA-repair activity in lung tissues (28). We used UV-irradiated DNA, which contains cyclobutane pyrimidine dimers as well as <6-4> photoproducts; Acr-modified DNA, which contains γ-OH-PdG; and H_2O_2-modified DNA, which contains 8-oxo-dG, as substrates (13, 28). It is well established that NER is the major mechanism that repairs cyclobutane pyrimidine dimers, <6-4> photoproducts, and γ-OH-PdG, and that BER is the major mechanism that repairs 8-oxo-dG (32, 33). Therefore, these two types of substrates allow us to determine the NER and BER activity in the cell lysates (11, 13). The results in Fig. 3 *A* and *B* and Fig. S2 show that both NER and BER activity in lung tissue of ECS-exposed mice are significantly lower than in lung tissue of filtered air (FA)-exposed mice.

ECS Causes a Reduction of Repair Protein XPC and OGG1/2. We then determined the level of XPC and OGG1/2, the two crucial proteins, respectively, for NER and BER (34, 35). The results in Fig. 3*C* show that the level of XPC and OGG1/2 in lung tissues of ECS-exposed mice was significantly lower than in control mice. We further determined the relationship between DNA adduct formation and DNA-repair activity in lung tissues of FA- and ECS-exposed mice. Since NER is the major repair mechanism for bulky DNA damage such as γ-OH-PdG and photodimers (11, 33) and BER is a major repair mechanism for base damage (32), we compared BER activity with the level of O^6-medG adducts and NER activity with the level of γ-OH-PdG adducts. The results in Fig. 3*D* show that NER and BER activity in lung tissue of different mice is inversely related to the level of γ-OH-PdG and O^6-medG adducts, respectively. These results indicate that in lung tissue, NER and BER activities are crucial factors in determining the level of ECS-induced γ-OH-PdG and O^6-medG DNA damage; mice that are more sensitive to ECS-induced DNA-repair inhibition accumulate more ECS-induced DNA damage in their lung and, perhaps, bladder and heart. It should be noted that in human cells, repair of O^6-medG adducts is mainly carried out by *O*^{6}-methylguanine DNA methyltransferase (MGMT) (36, 37). The positive relationship between BER activity and the O^6-medG level in lung tissues of mice implies that ECS impairs BER enzymes as well as MGMT, and/or O^6-medG is repaired by a BER mechanism in mice.

Nicotine Induces DNA Damage in Human Cells. Many tobacco-specific nitrosamines that result from the nitrosation of nicotine, such as NNN and NNK, are potent carcinogens and can induce cancer in different organs, including the lung (20, 21, 27). While NNK and NNN cannot covalently bind with DNA directly,

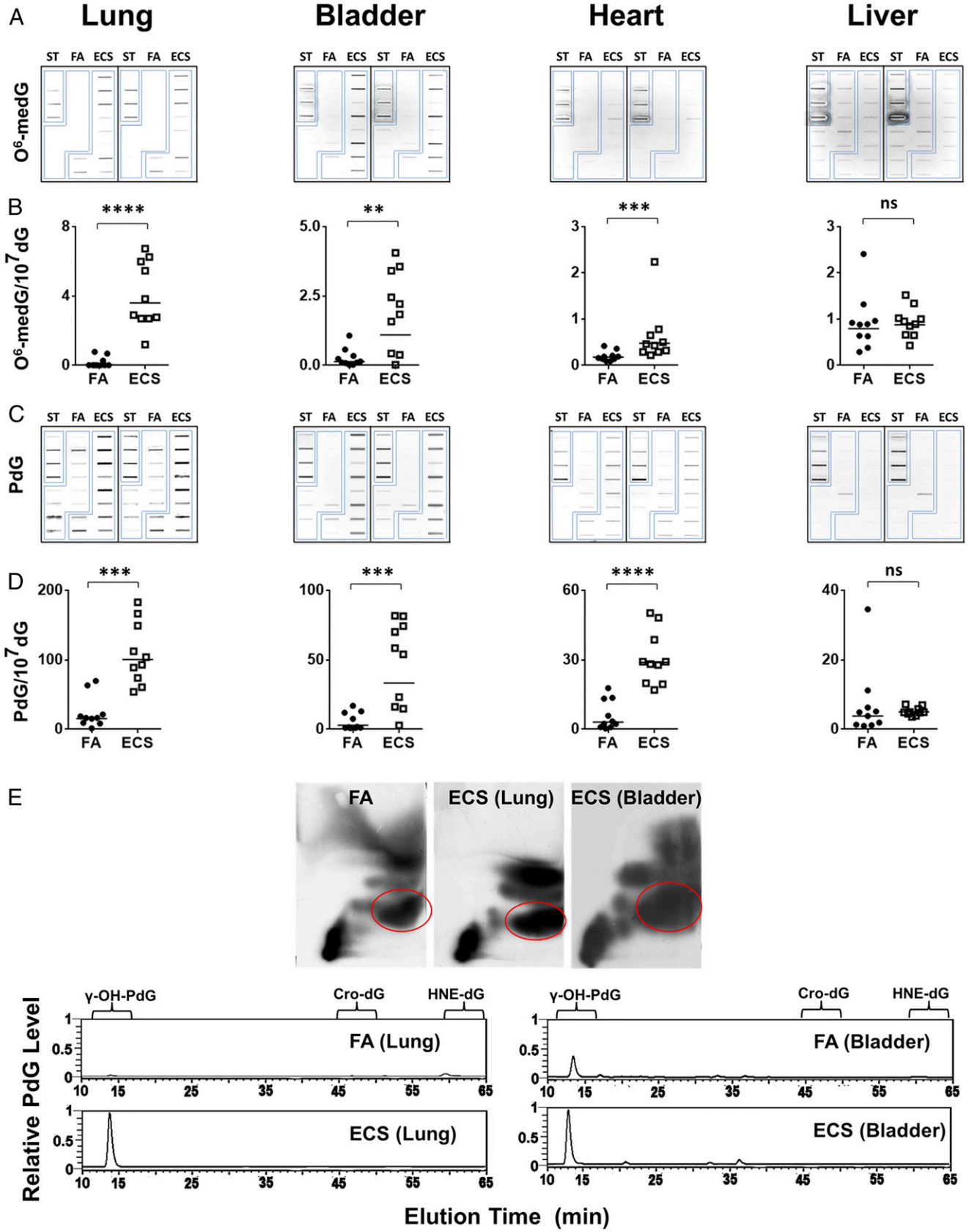

Fig. 1. ECS induces γ-OH-PdG and O^6-medG adducts in the lung, bladder and heart. Genomic DNA were isolated from different organs of mice exposed to FA or ECS as described in text. (*A*–*D*) O^6-medG and PdG formed in the genomic DNA were detected by immunochemical methods (28). (*A* and *C*) Slot blot. (*B* and *D*) Quantification results. The bar represents the mean value. (*E*) Identification of γ-OH-PdG adducts formed in the genomic DNA of lung and bladder by the 2D-TLC (*Upper*) and then HPLC (*Lower*) (28). ST, PdG, or O^6-medG standard DNA. ****$P < 0.0001$, ***$P < 0.001$, **$P < 0.01$, and *$P < 0.05$.

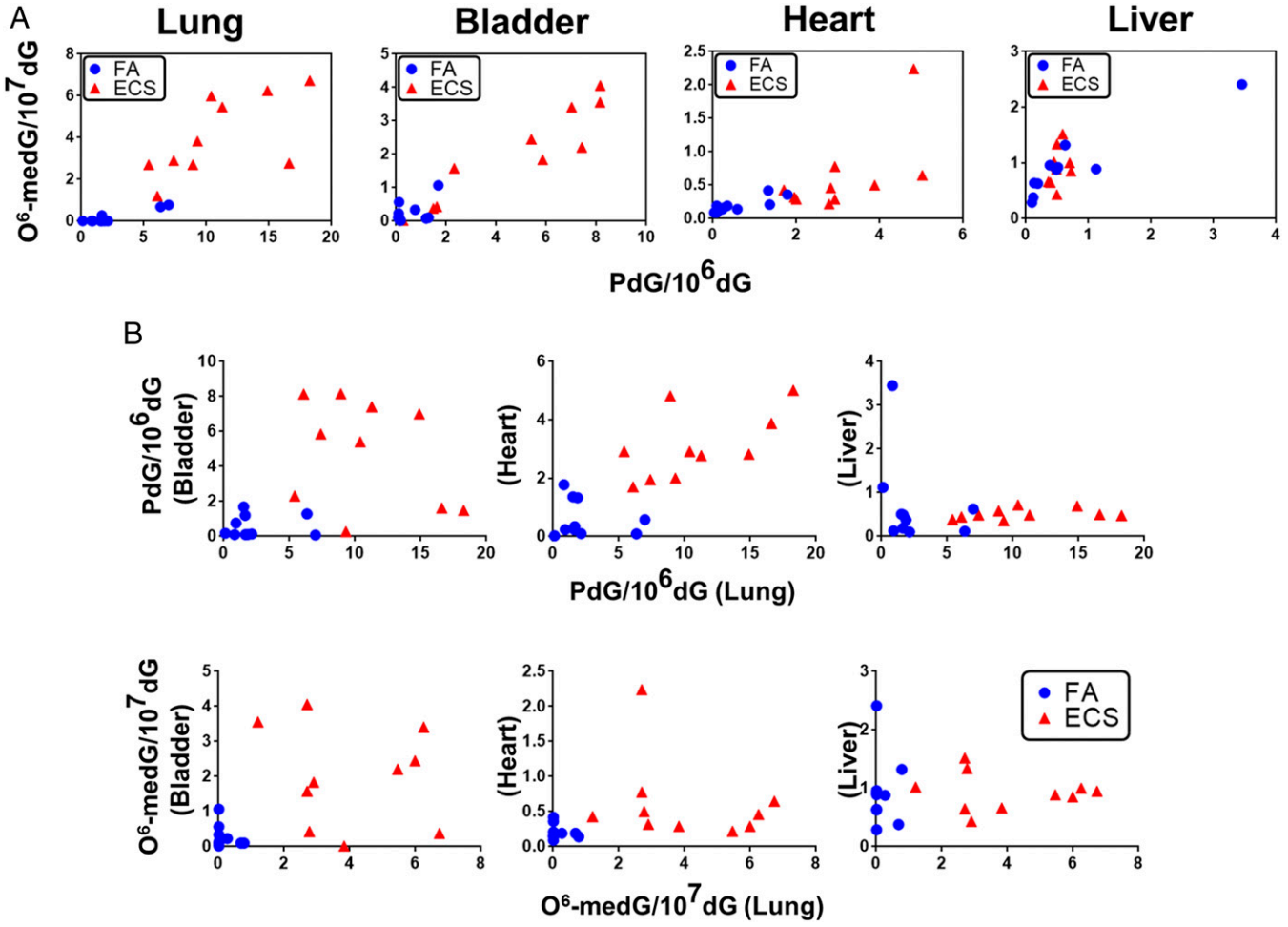

Fig. 2. Relationship of ECS-induced PdG versus O^6-medG formation in different organs of mice. The levels of PdG and O^6-medG detected in different organs from mice exposed to FA and ECS were determined in Fig. 1. In *A*, O^6-medG formation is plotted against PdG formation in each organ in mice exposed to ECS (red triangles) and FA (blue dots). In *B*, formation of PdG and O^6-medG in the bladder, heart, and liver is plotted against PdG and O^6-medG formation, respectively, in the lung of mice exposed to ECS and FA. Each symbol represents each individual mouse.

it has been proposed that one of NNK's metabolic products, MDOH, can interact with DNA to induce mutagenic O^6-medG adducts (20, 21, 27). These results raise the possibility that ECS-induced O^6-medG is due to the nitrosation of nicotine, and that NNK resulting from nicotine nitrosation then further transforms into MDOH in lung and bladder tissue (20). To test this possibility, we determined the DNA adducts induced by nicotine and NNK in cultured human bronchial epithelial and urothelial cells, and the effect of nicotine and NNK treatments on DNA repair, using the same methods indicated in Fig. 1. The results in Fig. 4 show that both nicotine and NNK can induce the same type of γ-OH-PdG adducts, and O^6-medG adducts. Since it is well established that many aldehydes can induce cyclic PdG in cells (38–40), these results suggest that aldehydes as well as MDOH are NNK metabolites, which induce γ-OH-PdG and O^6-medG.

Nicotine Reduces DNA Repair in Human Cells. We next determined the effects of nicotine and NNK treatment on DNA-repair activity and repair protein levels in human lung and bladder epithelial cells using the method described in Fig. 3. The results in Fig. 5 show that nicotine and NNK treatments not only inhibit NER and BER activities, they also reduce the protein levels of XPC and hOGG1/2. We found that these reductions of XPC and hOGG1/2 induced by nicotine and NNK can be prevented or attenuated by the proteasome and autophagosome inhibitors MG132, 3-methyladenine (3-MA), and lactacystin (Fig. S3) (13, 41–43). These results indicate that metabolites of nicotine and NNK can modify DNA-repair proteins and cause proteosomal and autophagosomal degradation of these proteins and that ECS's effect on the inhibition of DNA-repair activity is via modifications and degradation of DNA-repair proteins by its metabolites.

Together, these results indicate that human bronchial epithelial and urothelial cells as well as lung, heart, and bladder tissues in the mouse are able to nitrosate nicotine and metabolize nitrosated nicotine into NNK and then MDOH and aldehydes. Furthermore, whereas MDOH induces O^6-medG adducts, aldehydes not only can induce γ-OH-PdG, they also can inhibit DNA repair and cause repair protein degradation.

Nicotine Enhances Mutations and Cell Transformation. The aforementioned results demonstrate that ECS's major component nicotine, via its metabolites, MDOH, and aldehydes, not only can induce mutagenic DNA adducts, but that they also can inhibit DNA repair in human lung and bladder epithelial cells. These results raise the possibility that ECS and its metabolites can function not only as mutagens but also as comutagens to enhance DNA damage-induced mutagenesis. To test this possibility, we determined the effect of these agents on cell mutation susceptibility on UV- and H_2O_2-induced DNA damage

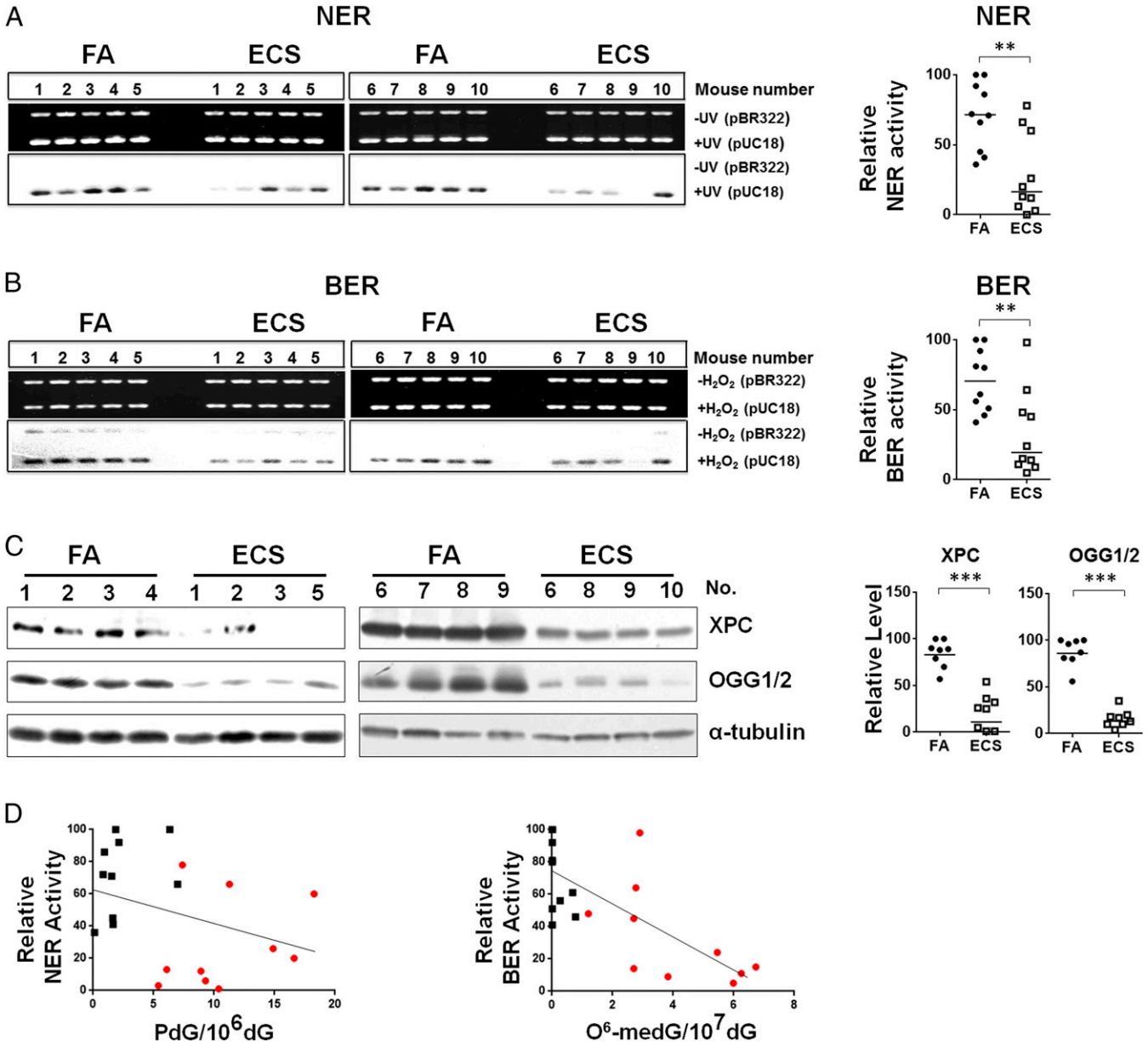

Fig. 3. ECS reduces DNA-repair activity and XPC and OGG1/2 in the lung. Cell lysates were isolated from lung tissues of mice exposed to FA ($n = 10$) or to ECS ($n = 10$) the same as in Fig. 1. The NER and the BER activity in the cell lysates were determined by the in vitro DNA damage-dependent repair synthesis assay as described (13, 28). (*A* and *B*) Ethidium bromide-stained gels (*Upper*) and autoradiograms (*Lower*) are shown in *Left*. In *Right*, the radioactive counts in the autoradiograms were normalized to input DNA. The relative repair activity was calculated using the highest band as 100%. (*C*) Detection of XPC and OGG1/2 protein in lung tissues ($n = 8$) by Western blot (*Left*). *Right* graphs are quantifications of ECS effect on the abundance of XPC and OGG1/2. The bar represents the mean value. (*D*) The relationship between the level of PdG and O^6-medG adduct and the NER and BER activity in lung tissues of FA- (black square) and ECS (red dot)-exposed mice.

using the well-established *supF* mutation system (13). The results in Fig. 6*A* show that nicotine and NNK treatment in both human lung and bladder epithelial cells enhances the spontaneous mutation frequency as well as UV- and H_2O_2-induced mutation frequency by two- to fourfold. These results indicate that nicotine and NNK treatment sensitize these human cells to the extent that they are more susceptible to mutagenesis. We further tested the effect of these agents on induction of tumorigenic transformation using the anchorage-independent soft-agar growth assay (44, 45). The results in Fig. 6 *B* and *C* show that nicotine and NNK greatly induce soft-agar anchorage-independent growth of human lung and bladder cells, a necessary ability for tumorigenic cells (46–49).

Discussion

The major purpose of E-cig smoking as well as tobacco smoking is to deliver the stimulant nicotine via aerosols, which allow smokers to obtain instant gratification. Unlike TS, which contains nitrosamines and numerous carcinogenic chemicals resulted from burning, ECS contains nicotine and relatively harmless organic solvents. Therefore, E-cig has been promoted as non-carcinogenic and a safer substitute for tobacco. In fact, recent studies show that E-cig smokers, similar to individuals on nicotine replacement therapy, have 97% less 4-(methylnitrosamino)-1-(3-pyridyl)-1-butanol (NNAL), an isoform form of NNK, a tobacco nitrosamine and lung carcinogen, in their body fluid

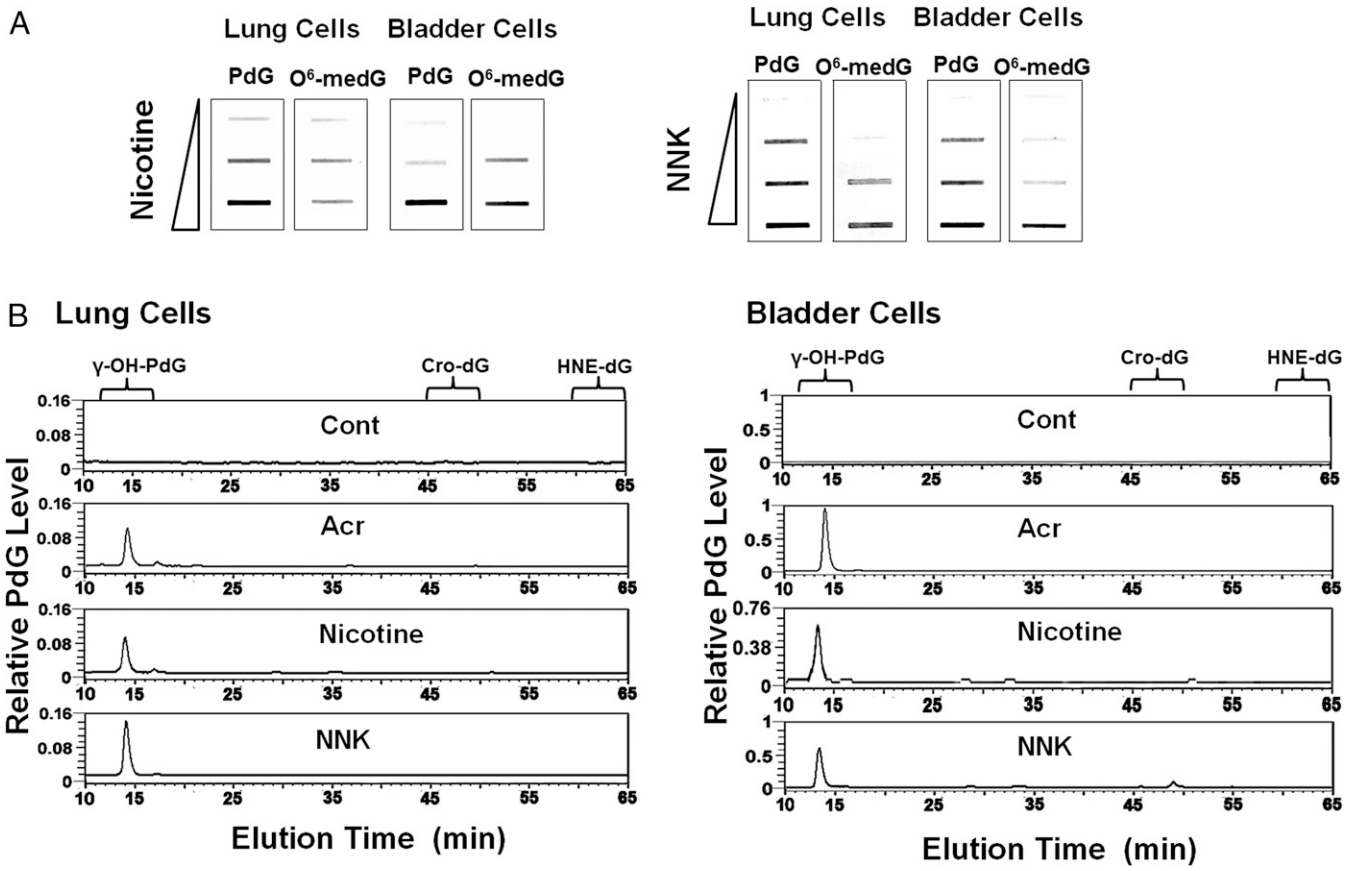

Fig. 4. Nicotine and NNK induce γ-OH-PdG and O^6-medG in cultured human lung and bladder epithelial cells. Human lung epithelial (BEAS-2B) cells and urothelial (UROtsa) cells were treated with different concentrations of nicotine and NNK as described in text. O^6-medG and PdG formed in the genomic DNA were determined as described in Fig. 1. (*A*) The DNA adducts were detected by immunochemical methods (13, 28). (*B*) The PdG adducts formed in the genomic DNA were further identified as γ-OH-PdG adducts by the ^{32}P postlabeling followed by 2D-TLC/HPLC method (13, 28).

than tobacco smokers (50). Based on these results, ECS has been recommended as a substitute for TS (50). However, E-cig smoking is gaining popularity rapidly particularly in young individuals and it is important to note that many of these E-cig smokers have taken up E-cig smoking habit are not necessary doing it for the purpose of quitting TS, rather, it is because they are assuming that E-cig smoking is safe. Currently, there are 18 million E-cig smokers in the United States and 16% of high school students smoke E-cig (51, 52). Understanding the carcinogenicity of ECS is an urgent public health issue. Since it takes decades for carcinogen exposure to induce cancer in humans, for decades to come there will be no meaningful epidemiological study to address the carcinogenicity of ECS. Therefore, animal models and cell culture models are the reasonable alternatives to address this question.

Nicotine has not been shown to be carcinogenic in animal models (7). However, during tobacco curing, substantial amounts of nicotine are transformed into tobacco-specific nitrosamines (TSA) via nitrosation, and many of these TSA, such as NNK and NNN, are carcinogenic in animal models (19, 53–55). Because of these findings, the occurrence and the level of nitrosamines in blood fluid have been used as the gold standard for determination of the potential carcinogenicity of smoking (56). While the NNAL level in E-cig smokers is 97% lower than in tobacco smokers, nonetheless, it is significant higher than in nonsmokers (50). This finding indicates that nitrosation of nicotine occurs in the human body and that ECS is potentially carcinogenic.

It is well established that cytochrome p450 enzymes in human and animal cells can metabolize and transform NNK, NNAL, and NNN into different products, which can modify DNA as well as proteins (20, 57, 58). This finding raises the possibility that the level of these nitrosamines detected in the blood stream of E-cig smokers at any given time may grossly underestimate the level of nicotine nitrosation. We undertake the approach of detecting DNA damage induced by nicotine rather than detecting nitrosamine level to address the potential mutagenic and carcinogenic effect of ECS. It should be noted that in vivo DNA damage can remain in genomic DNA for many hours and even days (13, 59, 60). Therefore, this approach not only is direct but also more sensitive in determining the carcinogenicity of ECS.

The level of γ-OH-PdG adducts induced by E-cig smoke in mice and by nicotine and NNK in cultured human cells is 10-fold higher than O^6-medG (Fig. 1). We have shown that γ-OH-PdG adducts are as mutagenic as BPDE-dG and UV photoproducts and induce G to T and G to A mutations similar to the mutations in the p53 gene in tobacco smoker lung cancer patients (11). Together, these results suggest that γ-OH-PdG adducts are the major cause of nitrosamine lung carcinogenicity.

The current understanding of NNK and NNN metabolism indicates that NNK metabolites are further transformed into PBDs, formaldehyde, and MDOH (20, 21, 61), while NNN metabolites are hydroxyl and keto forms of PBD (20, 21, 61). While MDOH can induce O^6-medG adducts, it is unclear what metabolites induce γ-OH-PdG adducts. It is well established that acrolein–DNA interaction generates γ-OH-PdG adducts (11, 13, 30) and that formaldehyde induces hydroxymethylated

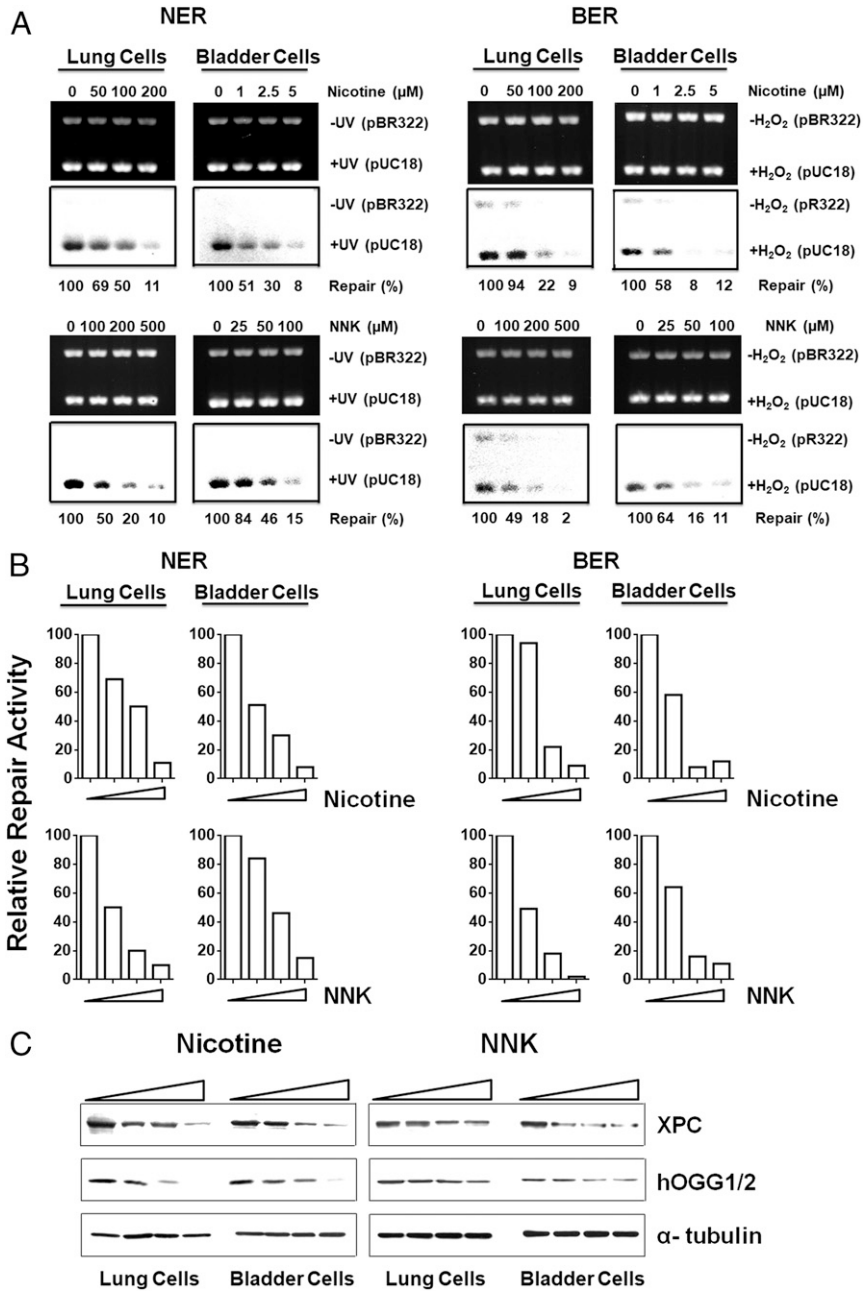

Fig. 5. Nicotine and NNK reduce DNA-repair activity and the level of repair proteins XPC and hOGG1/2 in cultured human lung and bladder epithelial cells. Cell-free cell lysates were isolated from human lung (BEAS-2B) and bladder epithelial (UROtsa) cells treated with different concentrations of nicotine and NNK 1 h at 37 °C. The NER and the BER activity in the cell lysates were determined by the in vitro DNA damage-dependent repair synthesis assay as described in Fig. 3. (*A*) Ethidium bromide-stained gels (*Upper*) and autoradiograms (*Lower*) are shown. (*B*) Quantifications results. The radioactive counts in the autoradiograms were normalized to input DNA. The relative repair activity was calculated using the control band as 100%. (*C*) The effect of nicotine and NNK treatment on abundance of XPC and hOGG1/2 in human lung and bladder urothelial cells were determined as described in Fig. 3.

nucleotides, mainly dG, in animal models (62). It has been found that in vitro formaldehyde combined with acetaldehyde can induce γ-OH-PdG (63). Therefore, it possible that ECS, nicotine, and NNK induce γ-OH-PdG via their metabolite formaldehyde, which triggers lipid peroxidation and produces acrolein and acetaldehyde byproducts; consequently, these byproducts induce γ-OH-PdG.

In summary, we found that ECS induces mutagenic γ-OH-PdG and O^6-medG adducts in lung, bladder, and heart tissues of exposed mice. ECS also causes reduction of DNA-repair activity and repair proteins XPC and OGG1/2 in lung tissue. Furthermore, nicotine and NNK induce the same effects in human lung and bladder epithelial cells. We propose that nicotine can be nitrosated, metabolized, and further transformed into aldehydes and MDOH in lung, bladder, and heart tissues of humans and mice. Whereas MDOH induced O^6-medG, aldehydes not only induce γ-OH-PdG, but also inhibit DNA repair and reduce XPC and OGG1 proteins (Fig. S3). We also found that nicotine and NNK can enhance mutational susceptibility and induced tumorigenic transformation of human lung and bladder epithelial cells. Based on these results, we propose that ECS is carcinogenic and that E-cig smokers have a higher risk

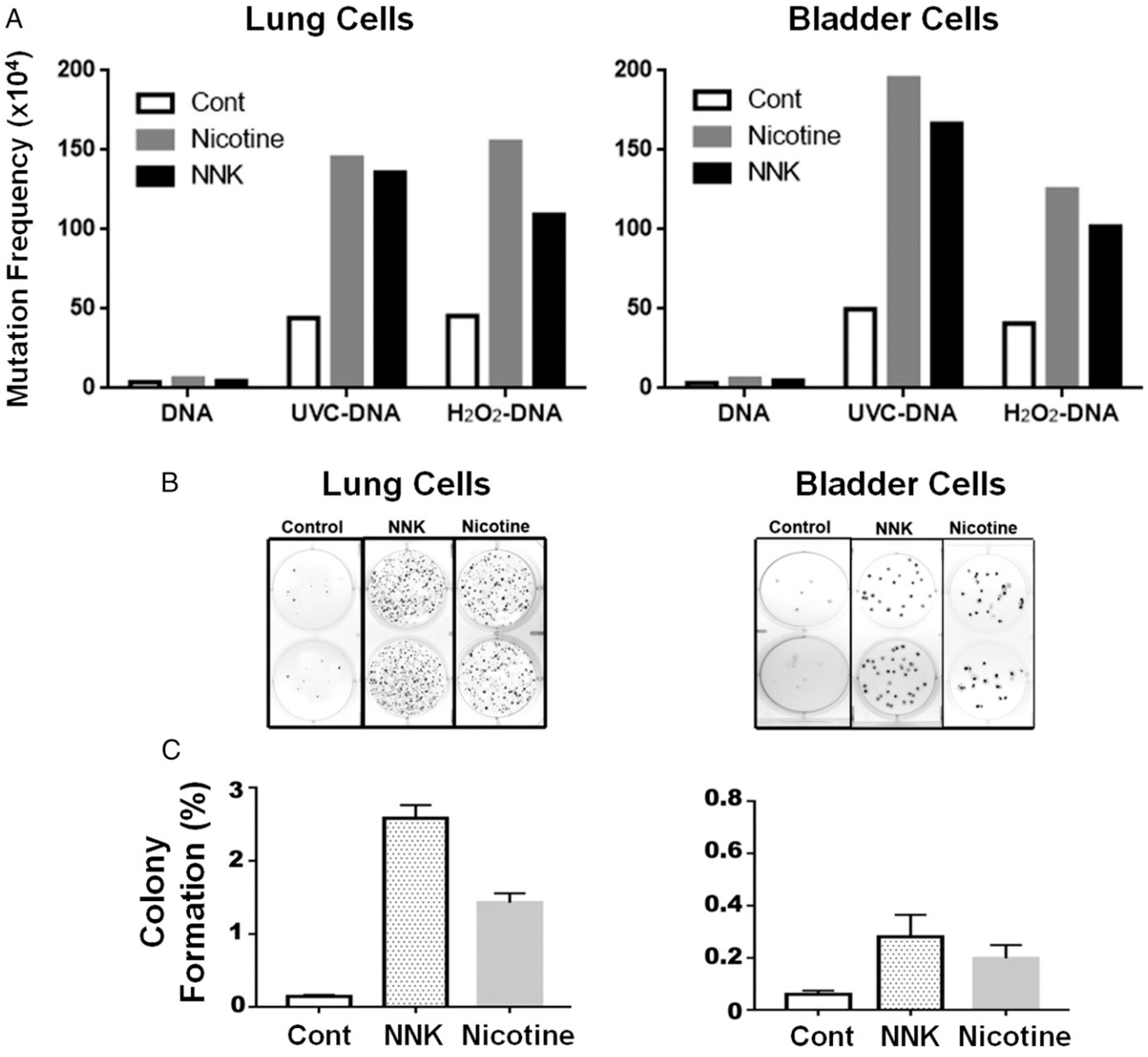

Fig. 6. Nicotine and NNK treatments enhance mutational susceptibility and cell transformation. Human lung and bladder epithelial cells (BEAS-2B and UROtsa) were treated with NNK (0.5 mM) and nicotine (25 mM for BEAS-2B cells, and 5 mM for UROtsa cells) for 1 h at 37 °C; these treatments render 50% cell killing. (*A*) UVC-irradiated (1,500 J/m^2) or H_2O_2 modified (100 mM, 1 h at 37 °C) plasmid DNAs containing the *supF* gene were transfected into these cells, and the mutations in control, and nicotine- and NNK- treated cells were detected and quantified as previously described (13, 28). (*B*) Detection of anchorage-independent soft-agar growth. A total of 5,000 treated cells were seeded in a soft-agar plate. The method for anchorage-independent soft-agar growth is the same as previously described (28). Typical soft-agar growth plates stained with crystal violet were shown. (*C*) Quantifications of percent of control, nicotine, and NNK-treated cells formed colonies in soft-agar plates.

than nonsmokers to develop lung and bladder cancer and heart diseases.

Materials and Methods

Materials. Acr-dG monoclonal antibodies and plasmid pSP189 were prepared, as described (13, 41). Acr-dG antibodies are specific for PdG adducts including Acr-, HNE-, and crotonaldehyde (Cro)-dG (29). Antibodies for XPC, hOGG1/2 (cross reacts with mouse OGG1/2), α-tubulin, and mouse/rabbit IgG; enzymes, T4 kinase, protease K, nuclease P, and RNase A; and chemicals, acrolein, nicotine, and NNK were commercially available. Immortalized human lung (BEAS-2B) and bladder epithelial (UROtsa) cells were obtained from American Type Culture Collection and J.R. Masters, University College London, London. All animal procedures were approved by the Institutional Animal Care and Use Committee, New York University School of Medicine.

ECS Generation and Mice Exposure. Twenty FVBN (Jackson Laboratory, Charles River) male mice were randomized into two groups, 10 each. Mice were exposed to ECS (10 mg/mL), 3 h/d, 5 d/wk, for 12 wk. ECS was generated by an E-cig machine, as previously described (64). An automated three-port E-cigarette aerosol generator (e∼Aerosols) was used to produce E-cigarette aerosols from NJOY top fill tanks (NJOY, Inc.) filled with 1.6 mL of e-juice with 10 mg/mL nicotine in a propylene glycol/vegetable glycerin mixture (50/50 by volume; MtBakerVapor MESA). Each day the tanks were filled with fresh e-juice from a stock mixture, and the voltage was adjusted to produce a consistent wattage (∼1.96 A at 4.2 V) for each tank. The puff aerosols were generated with charcoal and high-efficiency particulate filtered air using a

rotorless and brushless diaphragm pump and a puff regime consisting of 35-mL puff volumes of 4-s duration at 30-s intervals. Each puff was mixed with filtered air before entering the exposure chamber (1 m^3). Tanks were refilled with fresh e-juice at 1.5 h into the exposure period during the pause between puffs. Mass concentrations of the exposure atmospheres were monitored in real time using a DataRam4 (Thermo Fisher Scientific) and also determined gravimetrically by collecting particles on Teflon filters (Teflo, 2 mm pore size; Pall) weighed before and after sample collection using an electrobalance (MT-5; Metler).

Cell Cultures and Treatments of Nicotine and NNK. Exponentially growing BEAS-2B and UROtsa were treated with different concentrations of nicotine (BEAS-2B: 0, 100, 200 μM; UROtsa: 0, 1, 2.5 μM), and NNK (BEAS-2B: 0, 100, 300, 1,000 μM; UROtsa: 0, 50, 100, 200 μM) for determination of DNA adduct and DNA-repair activity. For XPC and hOGG1/2 detection, BEAS-2B were treated with nicotine (0, 50, 100, 200 μM), and NNK (0, 500, 750, 1,000 μM) and UROtsa were treated with nicotine (0, 1, 2.5, 5 μM) and NNK (0, 100, 200, 400 μM) for 1 h at 37 °C. Genomic DNA and cell lysate isolation from these cells was the same as described (28).

PdG and O^6-medG Adduct Detection. Cyclic PdG and O^6-medG adducts formed in the genomic DNA were determined by the immunochemical slot blot hybridization method using Acr-dG and O^6-medG antibodies and quantum dot labeled second antibody, as described (13, 28). PdG adducts formed in cultured human cells, and mouse lung tissue were further analyzed by the ^{32}P postlabeling-2D-TLC/HPLC method, as previously described (28).

In Vitro DNA-Damage-Dependent Repair Synthesis Assay. The DNA-repair activity was assessed by an in vitro DNA damage-dependent repair synthesis assay, as previously described (13).

DNA Repairs Proteins Detection. The levels of XPC and OGG1/2 proteins in lung tissues of mice with and without ECS exposure, and in BEAS-2B and UROtsa cells treated with nicotine and NNK, were determined, as described (13).

Mutation Susceptibility Determination. Shuttle vector pSP189 plasmids, which contain the tyrosine suppressor tRNA coding gene the *supF*, were UV (1,500 J/m^2) irradiated or modified with H_2O_2 (100 mM, 1 h at 37 °C), then transfected into cells with and without pretreated with nicotine and NNK for 1 h at 37 °C. Mutations in the *supF* mutations were detected, as previously described (13).

Anchorage-Independent Soft-Agar Growth. Lung (BEAS-2B) and bladder (UROtsa) epithelial cells were treated with NNK (0.5 mM) and nicotine (25 and 5 mM) for 1 h at 37 °C; these treatments rendered 50% cell killing. The method for anchorage-independent soft-agar growth is the same as previously described (28).

Statistical Analysis. Statistical analysis and graphs were performed with Prism 6 (GraphPad) software. Two group comparisons were conducted with the unpaired, two-tailed Mann–Whitney *u* test or the unpaired, two-tailed *t* test with Welsh's correction for unequal variances. A P value <0.05 was considered to be significant.

ACKNOWLEDGMENTS. We thank Drs. Frederic Beland and Catherine B. Klein for reviewing this manuscript and Ms. Mona I. Churchwell for technical assistance. This work was supported by National Institutes of Health Grants R01CA190678, 1P01CA165980, ES00260, and P30CA16087.

1. Farsalinos KE, Polosa R (2014) Safety evaluation and risk assessment of electronic cigarettes as tobacco cigarette substitutes: A systematic review. *Ther Adv Drug Saf* 5: 67–86.
2. Javed F, Kellesarian SV, Sundar IK, Romanos GE, Rahman I (2017) Recent updates on electronic cigarette aerosol and inhaled nicotine effects on periodontal and pulmonary tissues. *Oral Dis* 23:1052–1057.
3. Grana R, Benowitz N, Glantz SA (2014) E-cigarettes: A scientific review. *Circulation* 129:1972–1986.
4. Cheng T (2014) Chemical evaluation of electronic cigarettes. *Tob Control* 23:ii11–ii17.
5. Hecht SS (1999) Tobacco smoke carcinogens and lung cancer. *J Natl Cancer Inst* 91: 1194–1210.
6. NTP (National Toxicology Program) (2016) Report on carcinogens,14th Edition (US Department of Health and Human Services, Public Health Service, Research Triangle Park, NC). Available at http://ntp.niehs.nih.gov/go/roc14. Accessed March 10, 2017.
7. US Department of Health and Human Services (2014) *The Health Consequences of Smoking—50 Years of Progress: A Report of the Surgeon General* (US Department of Health and Human Services, Centers for Disease Control and Prevention, National Center for Chronic Disease Prevention and Health Promotion, Office on Smoking and Health, Atlanta).
8. US Department of Health and Human Services (2006) *The Health Consequences of Involuntary Exposure to Tobacco Smoke: A Report of the Surgeon General* (US Department of Health and Human Services, Centers for Disease Control and Prevention, Coordinating Center for Health Promotion, National Center for Chronic Disease Prevention and Health Promotion, Office on Smoking and Health, Atlanta).
9. O'Loughlin J, Wellman RJ, Potvin L (2016) Whither the e-cigarette? *Int J Public Health* 61:147–148.
10. Loeb LA, Loeb KR, Anderson JP (2003) Multiple mutations and cancer. *Proc Natl Acad Sci USA* 100:776–781.
11. Feng Z, Hu W, Hu Y, Tang MS (2006) Acrolein is a major cigarette-related lung cancer agent: Preferential binding at p53 mutational hotspots and inhibition of DNA repair. *Proc Natl Acad Sci USA* 103:15404–15409.
12. Feng Z, Hu W, Tang MS (2004) Trans-4-hydroxy-2-nonenal inhibits nucleotide excision repair in human cells: A possible mechanism for lipid peroxidation-induced carcinogenesis. *Proc Natl Acad Sci USA* 101:8598–8602.
13. Wang HT, et al. (2012) Effect of carcinogenic acrolein on DNA repair and mutagenic susceptibility. *J Biol Chem* 287:12379–12386.
14. Benowitz NL, Jacob P, 3rd (1994) Metabolism of nicotine to cotinine studied by a dual stable isotope method. *Clin Pharmacol Ther* 56:483–493.
15. Hecht SS (2002) Human urinary carcinogen metabolites: Biomarkers for investigating tobacco and cancer. *Carcinogenesis* 23:907–922.
16. Stepanov I, et al. (2009) Evidence for endogenous formation of N′-nitrosonornicotine in some long-term nicotine patch users. *Nicotine Tob Res* 11:99–105.
17. Knezevich A, Muzic J, Hatsukami DK, Hecht SS, Stepanov I (2013) Nornicotine nitrosation in saliva and its relation to endogenous synthesis of N′-nitrosonornicotine in humans. *Nicotine Tob Res* 15:591–595.
18. Benowitz NL, Hukkanen J, Jacob P, 3rd (2009) Nicotine chemistry, metabolism, kinetics and biomarkers. *Handb Exp Pharmacol* 29–60.
19. IARC (2007) *IARC Monographs on the Evaluation of Carcinogenic Risks to Humans* (Intl Agency Res Cancer, Lyon, France), Vol 89, pp 457–480.
20. Hecht SS (2003) Tobacco carcinogens, their biomarkers and tobacco-induced cancer. *Nat Rev Cancer* 3:733–744.
21. Hecht SS, Carmella SG, Foiles PG, Murphy SE, Peterson LA (1993) Tobacco-specific nitrosamine adducts: Studies in laboratory animals and humans. *Environ Health Perspect* 99:57–63.
22. Swenberg JA, et al. (2011) Endogenous versus exogenous DNA adducts: Their role in carcinogenesis, epidemiology, and risk assessment. *Toxicol Sci* 120:S130–S145.
23. Upadhyaya P, Kalscheuer S, Hochalter JB, Villalta PW, Hecht SS (2008) Quantitation of pyridylhydroxybutyl-DNA adducts in liver and lung of F-344 rats treated with 4-(methylnitrosamino)-1-(3-pyridyl)-1-butanone and enantiomers of its metabolite 4-(methylnitrosamino)-1-(3-pyridyl)-1-butanol. *Chem Res Toxicol* 21:1468–1476.
24. Peterson LA, et al. (2013) Role of aldehydes in the toxic and mutagenic effects of nitrosamines. *Chem Res Toxicol* 26:1464–1473.
25. Beland FA, Fullerton NF, Heflich RH (1984) Rapid isolation, hydrolysis and chromatography of formaldehyde-modified DNA. *J Chromatogr A* 308:121–131.
26. Bartsch H, Montesano R (1984) Relevance of nitrosamines to human cancer. *Carcinogenesis* 5:1381–1393.
27. Xue J, Yang S, Seng S (2014) Mechanisms of cancer induction by tobacco-specific NNK and NNN. *Cancers (Basel)* 6:1138–1156.
28. Lee HW, et al. (2015) Cigarette side-stream smoke lung and bladder carcinogenesis: Inducing mutagenic acrolein-DNA adducts, inhibiting DNA repair and enhancing anchorage-independent-growth cell transformation. *Oncotarget* 6:33226–33236.
29. Pan J, et al. (2012) Detection of acrolein-derived cyclic DNA adducts in human cells by monoclonal antibodies. *Chem Res Toxicol* 25:2788–2795.
30. Wang HT, et al. (2013) Effect of CpG methylation at different sequence context on acrolein- and BPDE-DNA binding and mutagenesis. *Carcinogenesis* 34:220–227.
31. Wang HT, Zhang S, Hu Y, Tang MS (2009) Mutagenicity and sequence specificity of acrolein-DNA adducts. *Chem Res Toxicol* 22:511–517.
32. David SS, O'Shea VL, Kundu S (2007) Base-excision repair of oxidative DNA damage. *Nature* 447:941–950.
33. Friedberg EC (2003) DNA damage and repair. *Nature* 421:436–440.
34. Sugasawa K, et al. (1998) Xeroderma pigmentosum group C protein complex is the initiator of global genome nucleotide excision repair. *Mol Cell* 2:223–232.
35. Radicella JP, Dherin C, Desmaze C, Fox MS, Boiteux S (1997) Cloning and characterization of hOGG1, a human homolog of the OGG1 gene of Saccharomyces cerevisiae. *Proc Natl Acad Sci USA* 94:8010–8015.
36. Tano K, Shiota S, Collier J, Foote RS, Mitra S (1990) Isolation and structural characterization of a cDNA clone encoding the human DNA repair protein for O6-alkylguanine. *Proc Natl Acad Sci USA* 87:686–690.
37. Natarajan AT, et al. (1992) Chromosomal localization of human O6-methylguanine-DNA methyltransferase (MGMT) gene by in situ hybridization. *Mutagenesis* 7:83–85.
38. Esterbauer H, Zollner H (1989) Methods for determination of aldehydic lipid peroxidation products. *Free Radic Biol Med* 7:197–203.
39. Guéraud F, et al. (2010) Chemistry and biochemistry of lipid peroxidation products. *Free Radic Res* 44:1098–1124.
40. Gentile F, et al. (2017) DNA damage by lipid peroxidation products: Implications in cancer, inflammation and autoimmunity. *AIMS Genet* 4:103–137.
41. Lee HW, et al. (2014) Acrolein- and 4-Aminobiphenyl-DNA adducts in human bladder mucosa and tumor tissue and their mutagenicity in human urothelial cells. *Oncotarget* 5:3526–3540.
42. Kraft C, Peter M, Hofmann K (2010) Selective autophagy: Ubiquitin-mediated recognition and beyond. *Nat Cell Biol* 12:836–841.

43. Schrader EK, Harstad KG, Matouschek A (2009) Targeting proteins for degradation. *Nat Chem Biol* 5:815–822.
44. Freedman VH, Shin SI (1974) Cellular tumorigenicity in nude mice: Correlation with cell growth in semi-solid medium. *Cell* 3:355–359.
45. Borowicz S, et al. (2014) The soft agar colony formation assay. *J Vis Exp* e51998.
46. Cressey D (2014) E-cigarettes affect cells. *Nature* 508:159.
47. Zhou H, Calaf GM, Hei TK (2003) Malignant transformation of human bronchial epithelial cells with the tobacco-specific nitrosamine, 4-(methylnitrosamino)-1-(3-pyridyl)-1-butanone. *Int J Cancer* 106:821–826.
48. Plesner BH, Hansen K (1983) Formaldehyde and hexamethylenetetramine in Styles' cell transformation assay. *Carcinogenesis* 4:457–459.
49. Heidelberger C, et al. (1983) Cell transformation by chemical agents–A review and analysis of the literature. A report of the US environmental protection agency genetox program. *Mutat Res* 114:283–385.
50. Shahab L, et al. (2017) Nicotine, carcinogen, and toxin exposure in long-term e-cigarette and nicotine replacement therapy users: A cross-sectional study. *Ann Intern Med* 166:390–400.
51. Coleman BN, et al. (2017) Electronic cigarette use among US adults in the population assessment of tobacco and health (PATH) study, 2013-2014. *Tob Control* 26: e117–e126.
52. Singh T, et al. (2016) Tobacco use among middle and high school students–United States, 2011-2015. *MMWR Morb Mortal Wkly Rep* 65:361–367.
53. Hecht SS, et al. (1978) Tobacco-specific nitrosamines: Formation from nicotine in vitro and during tobacco curing and carcinogenicity in strain A mice. *J Natl Cancer Inst* 60: 819–824.
54. Hecht SS, Adams JD, Numoto S, Hoffmann D (1983) Induction of respiratory tract tumors in Syrian golden hamsters by a single dose of 4-(methylnitrosamino)-1-(3-pyridyl)-1-butanone (NNK) and the effect of smoke inhalation. *Carcinogenesis* 4: 1287–1290.
55. Hecht SS, et al. (1986) Induction of oral cavity tumors in F344 rats by tobacco-specific nitrosamines and snuff. *Cancer Res* 46:4162–4166.
56. Carmella SG, et al. (1990) Mass spectrometric analysis of tobacco-specific nitrosamine hemoglobin adducts in snuff dippers, smokers, and nonsmokers. *Cancer Res* 50: 5438–5445.
57. Phillips DH (2002) Smoking-related DNA and protein adducts in human tissues. *Carcinogenesis* 23:1979–2004.
58. Hecht SS (1998) Biochemistry, biology, and carcinogenicity of tobacco-specific N-nitrosamines. *Chem Res Toxicol* 11:559–603.
59. Morris RJ, Fischer SM, Slaga TJ (1986) Evidence that a slowly cycling subpopulation of adult murine epidermal cells retains carcinogen. *Cancer Res* 46:3061–3066.
60. Denissenko MF, Pao A, Pfeifer GP, Tang M (1998) Slow repair of bulky DNA adducts along the nontranscribed strand of the human p53 gene may explain the strand bias of transversion mutations in cancers. *Oncogene* 16:1241–1247.
61. Hecht SS (1999) DNA adduct formation from tobacco-specific N-nitrosamines. *Mutat Res* 424:127–142.
62. Lu K, Gul H, Upton PB, Moeller BC, Swenberg JA (2012) Formation of hydroxymethyl DNA adducts in rats orally exposed to stable isotope labeled methanol. *Toxicol Sci* 126:28–38.
63. Cheng G, et al. (2003) Reactions of formaldehyde plus acetaldehyde with deoxyguanosine and DNA: Formation of cyclic deoxyguanosine adducts and formaldehyde cross-links. *Chem Res Toxicol* 16:145–152.
64. Zhao J, Pyrgiotakis G, Demokritou P (2016) Development and characterization of electronic-cigarette exposure generation system (Ecig-EGS) for the physico-chemical and toxicological assessment of electronic cigarette emissions. *Inhal Toxicol* 28: 658–669.

ACS SENSORS

Article

pubs.acs.org/acssensors

Automated 3-D Printed Arrays to Evaluate Genotoxic Chemistry: E-Cigarettes and Water Samples

Karteek Kadimisetty,[†] Spundana Malla,[†] and James F. Rusling*[,†,‡,§,∥]

[†]Department of Chemistry, University of Connecticut, Storrs, Connecticut 06269, United States

[‡]Institute of Material Science, Storrs, Connecticut 06269, United States

[§]Department of Surgery and Neag Cancer Center, UConn Health, Farmington, Connecticut 06032, United States

[∥]School of Chemistry, National University of Ireland at Galway, Galaway, Ireland

Supporting Information

ABSTRACT: A novel, automated, low cost, three-dimensional (3-D) printed microfluidic array was developed to detect DNA damage from metabolites of chemicals in environmental samples. The electrochemiluminescent (ECL) detection platform incorporates layer-by-layer (LbL) assembled films of microsomal enzymes, DNA and an ECL-emitting ruthenium metallopolymer in ~10 nm deep microwells. Liquid samples are introduced into the array, metabolized by the human enzymes, products react with DNA if possible, and DNA damage is detected by ECL with a camera. Measurements of relative DNA damage by the array assess the genotoxic potential of the samples. The array analyzes three samples simultaneously in 5 min. Measurement of cigarette and e-cigarette smoke extracts and polluted water samples was used to establish proof of concept. Potentially genotoxic reactions from e-cigarette vapor similar to smoke from conventional cigarettes were demonstrated. Untreated wastewater showed a high genotoxic potential compared to negligible values for treated wastewater from a pollution control treatment plant. Reactivity of chemicals known to produce high rates of metabolite-related DNA damage were measured, and array results for environmental samples were expressed in terms of equivalent responses from these standards to assess severity of possible DNA damage. Genotoxic assessment of wastewater samples during processing also highlighted future on-site monitoring applications.

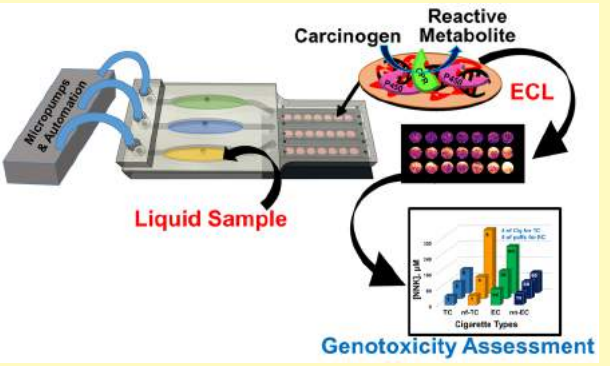

KEYWORDS: *3-D printing, genotoxicity, automation, e-cigarettes, environmental samples, electrochemiluminescence*

Genotoxicity refers to the ability of chemicals or their metabolites to interact with genetic material. Reactions with DNA include covalent adduct formation, oxidation, strand breaks, and noncovalent intercalations. When damage to DNA is not repaired, subsequent mutations occur that may lead to cancer.[1] For environmental chemicals and drugs, a battery of tests is typically used to predictively assess potential genotoxicity and other toxicities. Genotoxicity tests such as Comet, Ames, micronucleus, and mouse lymphoma assays are very useful for toxicity predictions, but are limited by ease of use and metabolic generality.[2] We previously developed microfluidic toxicity screening arrays with the ability to uncover multiple chemical pathways of genotoxicity by measuring DNA damage.[2] These high throughput electrochemiluminescent (ECL) and electrochemical assays include DNA and human metabolic enzymes that convert chemicals to metabolites, which are most often the DNA-reactive species in genotoxic pathways.[2]

Automated, disposable devices that rapidly detect genotoxic chemistry in environmental samples can serve to evaluate the potential influence of toxic chemicals and on-site risks to human health.[2,3] We recently reported a paper microfluidic device that estimated the genotoxic potential of water samples.[4] In this paper, 3-D printing is used to develop a more sophisticated and sensitive general automated array to assess genotoxic potential of environmental samples; 3-D printing was used to afford cheap, fast design and optimization. It has been used to print fluidic devices that detect pathogenic bacteria, biomedical markers, food allergens, and heavy metals, as well as in nanoparticle and chemical synthesis.[5,6] 3-D printed flow cells were designed for microdroplet generation, electrochemical sensing, and microfluidic devices.[7] We used desktop 3-D printers to develop devices for flow injection amperometry, flow cells to measure ECL,[8] and microfluidic immunoarrays to detect cancer biomarker proteins.[9]

The current device is designed for rapid assays of liquid samples. We focus here on two types of samples for reasons outlined below. The first is cigarette and e-cigarette smoke,

Received: February 27, 2017
Accepted: April 21, 2017
Published: April 21, 2017

DOI: 10.1021/acssensors.7b00118
ACS Sens. XXXX, XXX, XXX−XXX

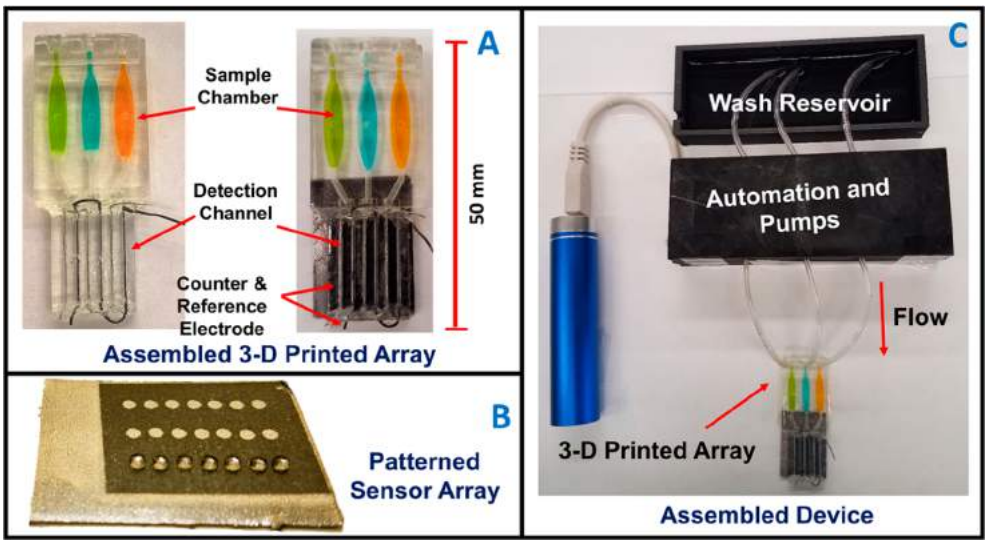

Figure 1. Automated genotoxicity screening array: (A) 3-D printed devices without (left) and with (right) microwell chip and counter electrode wires inserted showing the sample chambers containing dye solutions. (B) Microwell-patterned pyrolytic graphite detection array showing the first row holding 1 μL water droplets retained by the hydrophobic microwell boundaries. Each row is fed by a separate sample line. The working array features films of DNA, metabolic enzymes, and RuPVP in each microwell. (C) Assembled array system showing box enclosing electronic microprocessors and micropumps driven by a rechargeable battery and connected to the 3-D printed array below with a wash reservoir (top) containing pH 7.4 buffer.

since smoking is a major contributor to heart disease and cancer.[10] The second is contaminated water, a major public health concern.

Smoking causes more deaths than human immunodeficiency virus, illegal drug use, alcohol, motor vehicle accidents, and fire related deaths combined.[11] Electronic (e-)cigarettes are battery powered devices that vaporize nicotine, and were designed as an alternative to tobacco cigarettes. Additives in recent e-cigarettes make the vapor less harsh and allow more rapid delivery of nicotine to the brain, fostering use and increasing chances of addiction. Between 2011 and 2015 e-cigarette use increased from 1.5 to 16% among United States high school students and from 0.6 to 5.3% among middle school children.[12] In addition, e-cigarette vapor contains toxic metals such as cadmium, lead, and nickel at levels of 0.022−0.057 ng in 15 puffs of the aerosol.[13]

Currently one-third of available fresh water is used for agriculture, industrial and domestic purpose.[14] Chemical pollution of fresh water lakes and rivers is endemic in populated areas.[15] Toxic pollutants found in water bodies include nitrogenous and phosphorus species, organic chemicals, metals, and biologically generated compounds.[16] Coexistence of these chemicals in mixtures has been suggested as an origin of elevated genotoxic effects.[14,17]

In this paper, we report the first disposable, fully automated 3-D printed array designed to assess genotoxic potential of liquid environmental samples. This device can analyze vapor extract samples from cigarettes and water samples in 5 min for less than $1.00 (Figure 1). The arrays assess potential genotoxicity based on DNA reactivity of metabolites generated by enzymes on the array. To our knowledge, this is the first low cost 3-D printed microfluidic array capable of evaluating the metabolite-dependent genotoxic potential of environmental samples. Results suggest that e-cigarettes can have similar or enhanced genotoxic potential compared to tobacco cigarettes, depending on use patterns. The genotoxic potential of untreated wastewater was high, but was decreased to very low levels by reclamation in a sewage treatment facility.[18]

MATERIALS AND METHODS

Safety note: Benzo[*a*]pyrene (B[*a*]P), 4-[methyl(nitroso)amino]-1-(3-pyridinyl)-1-butanone (NNK), *N*′-nitroso-2-(3-pyridyl)pyrolidine (NNN), 2-acetylaminofluorene (2-AAF), 2-naphthylamine (2-NA), aflatoxin-B_1 (AFB1) and their metabolites are potential carcinogens. Handling these chemicals involved protections including gloves, safety glasses, and working in a hood.

Chemicals and Materials. B[*a*]P (MW 252.31), NNK (MW 207.23), NNN (MW 177.20), 2-AAF (MW 223.28), 2-NA (MW 143.19), AFB1 (MW 312.28), poly(diallyldimethylammonium chloride) (PDDA, avg MW = 100 000−200 000), poly(acrylic acid) (PAA, avg MW = 1800), calf thymus DNA (Type I), and other chemicals were from Sigma-Aldrich. Pooled male human liver microsomes were from BD Gentest. $[Ru(bpy)_2(PVP)_{10}]^{2+}$ {RuPVP; (bpy = 2,2-bipyridyl; PVP = poly(4-vinylpyridine)} was synthesized and characterized as described previously.[19] Pyrolytic graphite (PG) sheets are from Panasonic PGS-P13689-ND 70 μm thick.

3-D Printed Microfluidic Arrays. Microfluidic arrays were printed from clear acrylate resin using a Formlabs Form1+ stereolithographic 3-D printer. Design files are available on our Web site.[20] Briefly, CAD files incorporating the design were converted to printer instruction files for input to the printer (details in the Supporting Information (SI)). After printing, devices were rinsed internally and externally successively with isopropanol and water, then spray coating with clear acrylic spray (Krylon).

Arrays were printed with three sample chambers that feed three detection channels designed so that sample solutions flow directly across shallow 1 mm wide, 10 nm deep microwells on the detection chip to facilitate reactions with enzyme/DNA films in the wells (Figures 1A,B and S1). Detection chips were made from conductive pyrolytic graphite (PG) sheets cut to desired sizes. PG sheets were patterned with microwells using our print and peel technology[21] to accommodate tiny volumes of reagents during layer-by-layer (LbL) film assembly (Figure 1B).[22] A microwell template featuring 21 spots of diameter 1 mm in 3 rows with 7 spots per flow channel was inkjet printed onto glossy paper (Avery 5263) and heat pressed for 45 s at 275 °C to transfer onto these PG sheets (SI Figure S2, SEM).

DOI: 10.1021/acssensors.7b00118
ACS Sens. XXXX, XXX, XXX−XXX

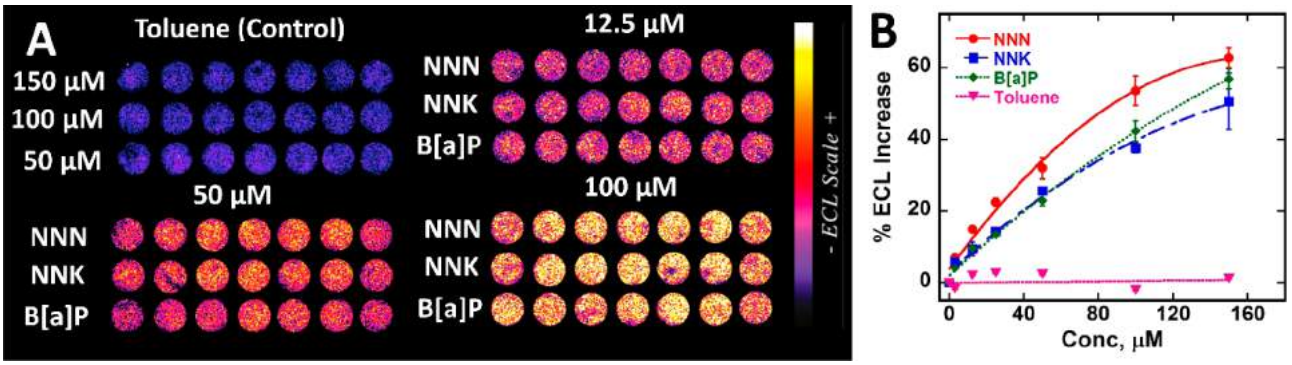

Figure 2. Array results for tobacco-related standards with DNA-reactive metabolites: (A) recolorized ECL data using arrays featuring RuPVP/enzyme/DNA microwells treated with oxygenated solutions of carcinogens B[*a*]P, NNK, and NNN and negative control toluene in 1% DMSO + 10 mM phosphate buffer pH 7.4 for 45 s at −0.65 V vs Ag/AgCl, with ECL captured by CCD camera after subsequently applying 1.25 V vs Ag/AgCl for 180 s. (B) Calibration plots of % ECL increase over 1% DMSO control vs concentration of standards. ECL intensity increases proportional to DNA damage that disorders ds-DNA and allows coreactant guanines in the DNA better access to Ru^{III} sites of RuPVP.[2]

Patterned PG sheets were attached onto the 3-D printed array using double sided adhesive.

Array were 3-D printed in less than 1 h using 6 mL of resin at fabrication cost $0.80. They have dimensions 50 mm (length (*L*)) × 22 mm (width (*W*)) × 5 mm (height (*H*)). Sample chamber dimensions are 17 mm (*L*) × 5 mm (*W*) × 2.5 mm (*H*) and maximum sample or reagent volume 170 ± 5 μL. Sample volume was 150 μL, and detection channels are 23 mm (*L*) × 3 mm (*W*) × 0.65 mm (*H*) with volume 45 ± 5 μL, and are provided with holes and grooves to accommodate stainless steel wire counter (0.4 mm diameter) and Ag/AgCl wire reference (0.6 mm diameter) electrodes to complete the ECL electrochemical detection cell (Figure 1A).

Automation. Automation was achieved by interfacing three Mp6 micropumps (Bartels) with an "ATtiny85" microprocessor chip via Bartels OEM microcontrollers (Figures S1 and S3). Micropump control features printed-circuit board (PCB)-linked microcontrollers independently connected to the ATtiny85 chip. The inexpensive 8-bit ATtiny microcontroller chip runs Arduino programs for pump control at low power consumption (Figure S3),[23] and provides ON/OFF commands to control voltage input to micropumps from a rechargeable lithium ion battery. Micropumps were adjusted to flow rate 120 ± 3 μL/min.

Layer by Layer Film Assembly. Sequential layers of ECL metallopolymer RuPVP, human liver microsome (HLM) enzyme source, and DNA were grown in microwells on the PG chip by layer-by-layer (LbL) alternate electrostatic assembly,[22] depositing appropriate solutions sequentially and incubating 20 min for polyion layers and 30 min for enzyme and DNA layers at 4 °C with water washing between adsorption steps.[24] Film architecture optimized for best signal/noise was PDDA/PAA/$(RuPVP/DNA)_2$/RuPVP/enzyme/DNA.

Detection of Genotoxic Reactions. The assay protocol involves two steps. First, the natural cyt P450 catalytic cycle is activated by applying −0.65 V vs Ag/AgCl while flowing oxygenated solutions of test samples in 10 mM phosphate buffer pH 7.4 + 1% DMSO for 45 s. This generates metabolites from the test compounds that can react with DNA.[25] Second, after washing the array with buffer, 1.25 V vs Ag/AgCl is applied for 180 s to generate ECL proportional to damage of coreactant DNA. This oxidizes $Ru^{II}PVP$ to $Ru^{III}PVP$, and $Ru^{III}PVP$ reacts with guanine in a complex pathway to form excited state $*Ru^{II}PVP$ that emits ECL light at 610 nm which is captured with a CCD camera in a dark box.[2] ECL generation involves oxidation of guanine by $Ru^{III}PVP$ in catalytic pathway resulting in a guanine radical that further reacts with $Ru^{III}PVP$ to form $*Ru^{II}PVP$ that emits light.[19] Covalent metabolite-nucleobase adducts disrupt the DNA double helix and can also lead to abasic sites and strand breaks, all resulting in more accessible guanines that generate more ECL. Electrodes are disposable and are discarded after each use.

Prior to assays, sample chambers (Figure 1A) were prefilled with 150 μL of test solution through sample injection ports, which are then sealed. Micropumps are connected to inlets with common feed at the back from a buffer reservoir (Figure 1C). Voltage input was by a three-electrode hand-held potentiostat. The entire device resides inside a dark box. Initially pumps are off, then the program initiates a 135 s pumping cycle for three steps, 10 s filling the detection channel, 45 s electrolysis, and 80 s washing. Samples were pumped into the 3 separate detection channels and 45 s electrolysis was done at −0.65 V vs Ag/AgCl once channels were full (while continuing flow) to activate the natural catalytic cycle of cyt P450s.,[25] After a subsequent 80 s wash cycle, pumps turn off and visible ECL light is generated by applying 1.25 V vs Ag/AgCl for 180 s and capturing light with a CCD camera. Timing was optimized for the best ECL signal/noise.

Sample Analyses. Smoke (vapor) extracts from e-cigarettes and filtered and nonfiltered tobacco cigarettes were collected using an artificial inhalation device (see the SI, Figure S4). Tubing connecting a syringe and the cigarette or e-cigarette was attached via a pipet tip plugged with cotton so that smoke passes through it and chemicals are trapped. This cotton was subsequently extracted with 2 mL of DMSO. To keep experimental conditions representative and relevant for vaping usage by smokers we extracted 100 puffs and smoke from 5 tobacco cigarettes for comparison. Vaping anywhere from 75 to 175 puffs from e-cigarettes is equivalent on average to 5−6 tobacco cigarettes per day.[26] Approximately 15−30 puffs from an e-cigarette is considered equivalent to smoke from one tobacco cigarette.[13,28]

Polyaromatic hydrocarbons and tobacco specific nitrosamines 4-(methylnitrosamino)-1-(3-pyridyl)-1-butanone (NNK) and *N*′-nitrosonornicotine (NNN) are major carcinogens present in cigarette smoke.[27] Most chemicals in tobacco cigarettes and e-cigarettes are similar to slightly lower concentrations reported for e-cigarettes.[13,28] Usually, contents of e-cigarettes are loaded into a cartridge and used with a battery operated inhalation device that heats and converts a nicotine solution with additives into an aerosol.[13] The contents of the e-cigarette liquid quoted by manufacturer content lists show tobacco derived nicotine, propylene glycol, vegetable glycerin, and natural and artificial flavoring agents.

Our second test targets featured untreated sewage water, partially, treated water and completely treated reclaimed water as collected from University of Connecticut water pollution control facility.[18] Water samples were passed through a 0.2 μM syringe filters (Thermo Scientific F2504-6) prior to genotoxic evaluation to remove particulate matter. Genotoxic chemicals present in wastewater 2-acetylaminofluorene (2-AAF),[29] 2-naphthylamine (2-NA),[30] and aflatoxin-B_1 (AFB1)[31] were used as reference standards.

RESULTS

Cigarettes and E-Cigarettes. Responses to tobacco smoke components B[*a*]P, NNK, and NNN were measured first. One

DOI: 10.1021/acssensors.7b00118
ACS Sens. XXXX, XXX, XXX−XXX

Scheme 1. Cytochrome P450 Mediated Bioactivation and DNA Reactivity of Standard Chemicals Used for Cigarette Studies[a]

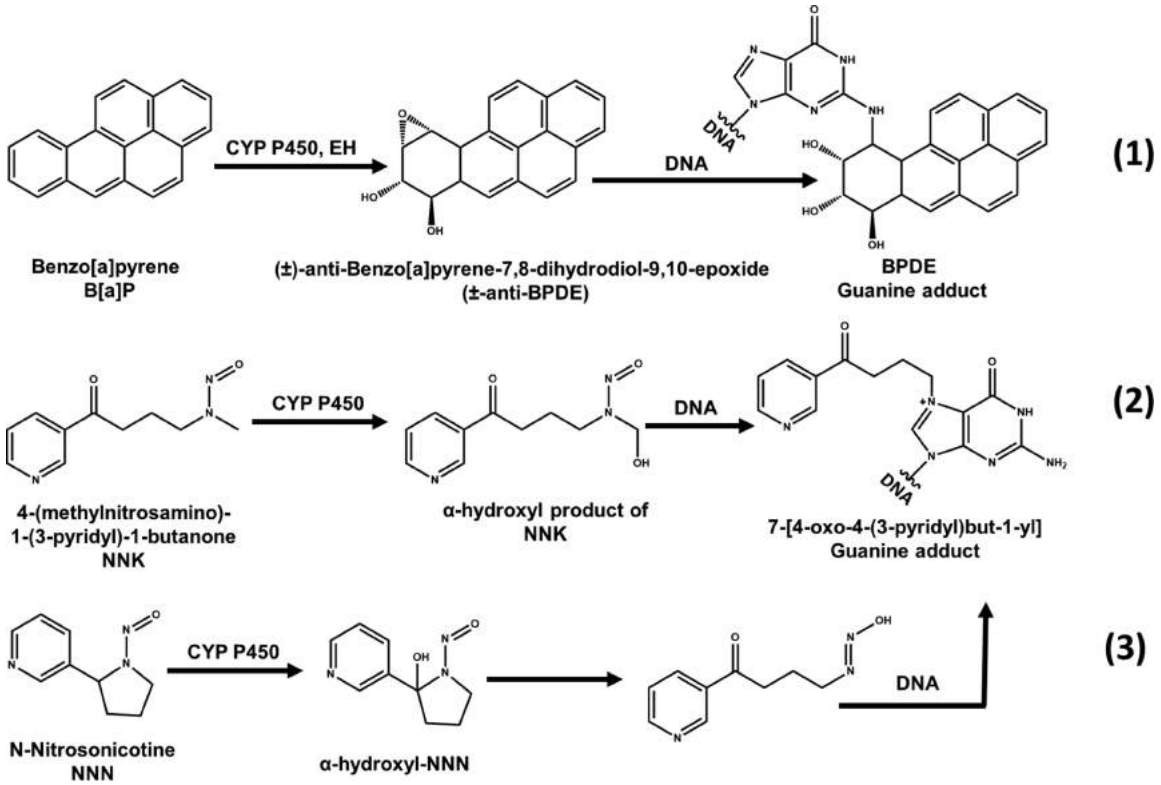

[a](1) Benzo[*a*]pyrene (B[*a*]P), metabolized to benzo[*a*]pyrene-7,8-dihydrodiol-9,10-epoxide that intercalates and covalently binds predominantly with guanine base in DNA, Adapted from information in ref 33. (2) 4-(Methylnitrosoamino)-1-(3-pyridyl)-1-butanone (NNK) and (3) *N*-nitrosonicotine (NNN) form hydroxyl forms before binding to nucleobases within DNA. Adapted from information in ref 34.

channel in the microfluidic array was used for each specific compound (Figure 2A). Plots of % ECL increase over the blank (1% DMSO in 10 mM phosphate buffer, pH 7.4) vs concentration of standard (Figure 2B) serve as standard calibration curves and their slopes reflect relative rates of DNA damage.[2] Dynamic range was from 3 to 150 μM for all standards. Increase in ECL intensity was observed with increase in test chemical concentration (Figure 2). ECL increases in earlier versions of related genotoxicity arrays were confirmed as directly related to amounts of specific metabolite-DNA adducts detected by LC-MS/MS.[2,4,24] In the present array, spot-to-spot variability was ±6% (n = 21) and array-to-array variability was ±7% (n = 3) (Figure S5). Toluene, with poorly DNA-reactive metabolites,[32] was used as a negative control with negligible ECL change (Figure 2).

Previous studies of B[a]P, NNK and NNN confirmed that reactive metabolites of these pro-carcinogens react with DNA to form covalent DNA adducts (Scheme 1). B[*a*]P is a polyaromatic hydrocarbon present in coal tar, cigarette smoke, and grilled meat. Metabolic cyt P450s catalyze B[*a*]P oxidation to a 7,8-epoxide that is rapidly hydrolyzed to a diol by epoxide hydrolase. The diol is further oxidized by cyt P450 to an epoxide to form ±-antibenzo[a]pyrene-7,8-dihydrodiol-9,10-epoxide (±-anti-BPDE, eq 1).[33] Major metabolite ±-anti-BPDE is classified as a Group I carcinogen by the International Agency of Research on Cancer (IARC). It is a strong electrophile that reacts with DNA nucleobases of to form covalent adducts. The major covalent adduct is formed by ±-anti-BPDE reaction with the exocyclic amine of nucleobase guanine to form a stable covalent adduct (Scheme 1, eq 1). Similarly, the tobacco specific nitroso amines NNK and NNN undergo α-hydroxylation catalyzed by cyt P450s to form reactive metabolites that react with DNA to form adducts at the N7 position of guanine (Scheme 1, eqs 2 and 3).[2,34,35]

Cigarette smoke and E-cigarette vapor trapped in the inhalation device (see Materials and Methods, and Figure S4, SI) was extracted into DMSO and then diluted 100-fold in pH 7.4 buffer prior to analysis. Vapor extract from 20 puffs of e-cigarettes was taken as equivalent to smoke from one tobacco cigarette.[13,28] We found large increases in ECL intensity with increases in amount of extracted cigarette smoke and e-cigarette vapor (Figure 3A), suggesting increased amounts of DNA damage[2,4] (Figure 3A,B). The most important finding is that % ECL values for equivalent numbers of puffs are slightly larger for e-cigarettes than for tobacco cigarettes, and much larger than for filtered tobacco cigarettes and non-nicotine e-cigarettes. These differences are significant at 95% confidence levels (t tests) and suggest that chemicals in the vapor of nicotine e-cigarettes metabolized in the array are at least as DNA-reactive as those in smoke of unfiltered tobacco cigarettes.

The difference in %ECL increase between filtered and nonfiltered tobacco cigarettes for 20 puff e-cigarette equivalents was not statistically different at the 95% confidence interval. However, for 60 and 100 e-cigarette puff equivalents, %ECL was statistically larger for unfiltered cigarettes at the 95% confidence level (Figure 3B). DNA reactivity of the non-nicotine e-cigarettes and the filtered tobacco cigarettes denoted by array signals were comparable, and ∼1.8-fold smaller than that for unfiltered tobacco cigarettes.

DOI: 10.1021/acssensors.7b00118
ACS Sens. XXXX, XXX, XXX−XXX

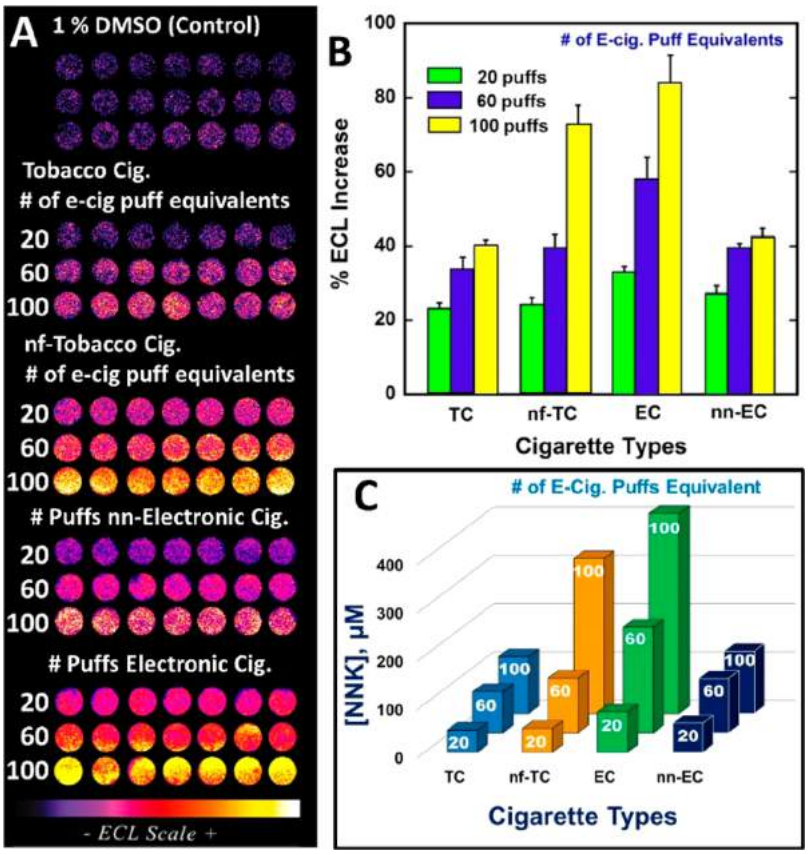

Figure 3. ECL array results comparing extracted vapor from e-cigarettes with extracted smoke from tobacco cigarettes using the conversion that 20 e-cigarette puffs equals smoke from one tobacco cigarette {Abbrev.: tobacco cigarettes (TC), e-cigarettes (EC), nonfiltered (nf) and non-nicotine (nn)}. (A) Recolorized ECL data from arrays. Each row represents microwells containing RuPVP/Enzyme/DNA layers treated with smoke extracted from 1, 3, and 5 TC and nf-TC (equivalent to 20, 60, and 100 puffs of e-cigarette) and 20, 60, and 100 puffs of EC and non-nicotine (nn)-EC in 1% DMSO containing buffer for 45 s under potential of −0.65 V vs Ag/AgCl. ECL captured while applying 1.25 V vs Ag/AgCl for 180 s. (B) % ECL increase over control (1% DMSO in buffer) vs cigarette samples. (C) NNK equivalents from %ECL for different cigarette samples.

To link these results to known DNA-reactive chemical metabolites, DNA-reactivity of the samples was expressed in terms of array responses of known tobacco component concentrations of B[*a*]P, NNK, and NNN using Figure 2B. This approach puts the results on a common footing related to major genotoxic components in tobacco smoke. Figure 3C shows the NNK-equivalent concentration in each of the cigarette types and suggest that nicotine e-cigarettes and unfiltered cigarettes are equivalent to quite significant levels of the potent tobacco carcinogen NNK. Equivalence of sample responses in terms of B[*a*]P and NNN are reported in Table S1 in the SI, and lead to qualitatively similar conclusions.

Water Samples. Known water pollutants 2-AAF, 2-NA, AFB1 were first tested as reference standards to assess genotoxic potential. Aflatoxins are metabolites of fungal organisms in polluted food and environmental samples and are associated with liver cancer.[36] Aflatoxin B1 is one of the most potent aflatoxins, and requires cyt P450 bioactivation to become carcinogenic. It is oxidized by cyt P450s to the 8,9-epoxide, which reacts with the N7 position of guanine to form covalent adducts (Scheme 2, eq 4).[37] Arylamines are commonly associated with bladder cancer.[38] 2-acetylaminofluorene (2-AAF) and 2-naphthylamine are converted by sequential reactions catalyzed by cyt P450s and acetyl transferase to arylnitrenium ions that react with nucleobases of DNA to form covalent adducts. A major adduct on the C8 position of guanine is shown in Scheme 2 (eqs 5, 6).[35,39,40]

Array results for these three compounds and toluene negative control are shown in Figure 4A. Plots of %ECL increase over blank (1% DMSO in pH 7.4 buffer) vs concentration of standard (Figure 4B) serve as calibration curves for water samples. Again, slopes reflect relative rates of DNA damage.[2] Dynamic ranges were from 3 to 100 μM. Limits of detection as %ECL increase 3× the avgerage noise were ∼3 μM for these genotoxic compounds.

Samples from the University of Connecticut water treatment facility were assayed on the array. Figure 4C shows a significant increase in ECL for untreated water samples compared to reclaimed and partially treated water samples. Results from Figure 4C are also expressed in terms of equivalent concentrations of the reference standards (Figure 4D) to provide comparisons of the relative genotoxicity potential of the samples. For example, the untreated wastewater is equivalent to about 10 μM of the parent chemical 2-AAF.

Compared to the untreated wastewater, the difference from the treated reclaimed water is significant at the 95% confidence level. Results suggest that more potentially genotoxic chemicals in the untreated wastewater are converted on the array to metabolites that are reactive with DNA compared to reclaimed or partially treated water samples. The larger %ECL for partially treated water compared to fully reclaimed water was also statistically significant at 95% confidence (Figure 4C, D). Genotoxic potential in terms of DNA reactivity of untreated

DOI: 10.1021/acssensors.7b00118
ACS Sens. XXXX, XXX, XXX−XXX

Scheme 2. Cytochrome P450 Mediated Bioactivation and DNA Reactivity of Standard Chemicals Used for Water Samples[a]

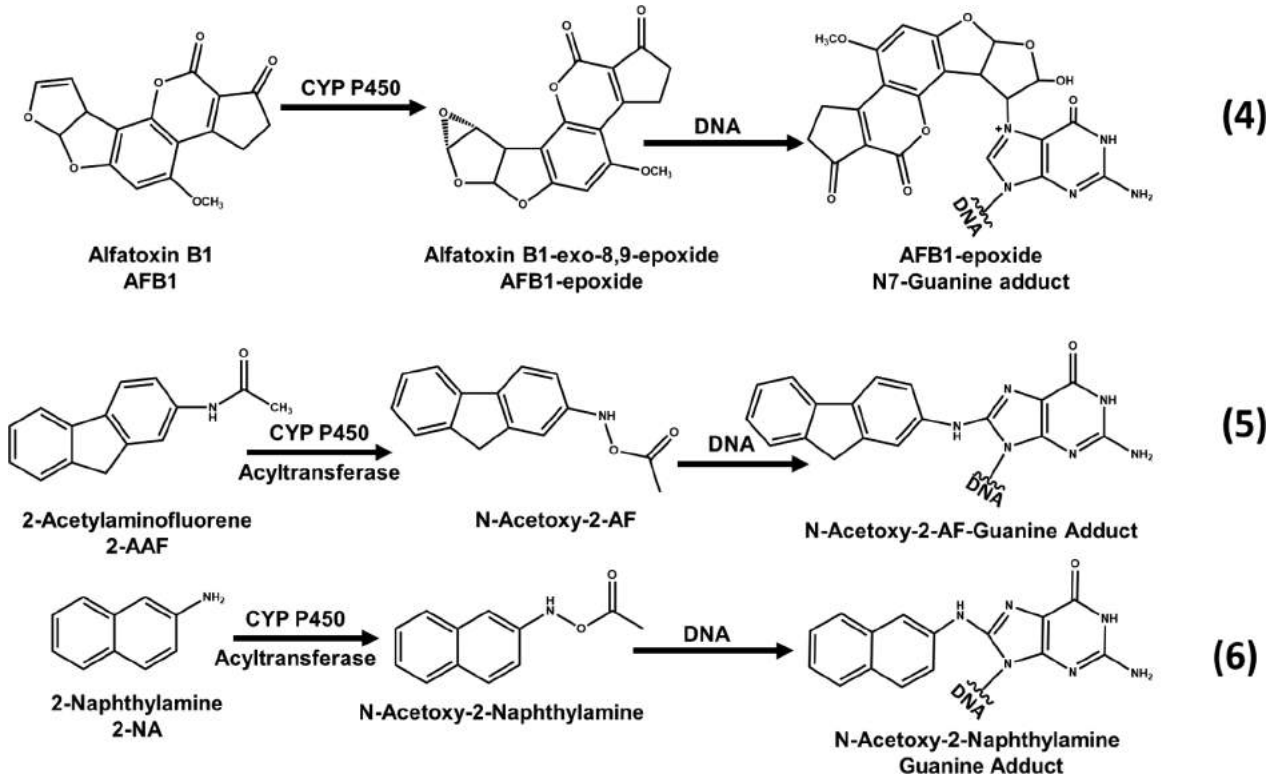

[a](4) Aflatoxin B1 (AFB1), metabolically activated to its epoxide form that forms covalent adducts with DNA nucleobases. Adapted from information in ref 37. (5) 2-Acetylaminofluorene (2-AAF). Adapted from information in ref 38. (6) 2-naphthylamine (2-NA) form acetoxy forms upon bioactivation that form covalent adducts with DNAnucleobases. Adapted from information in ref 40.

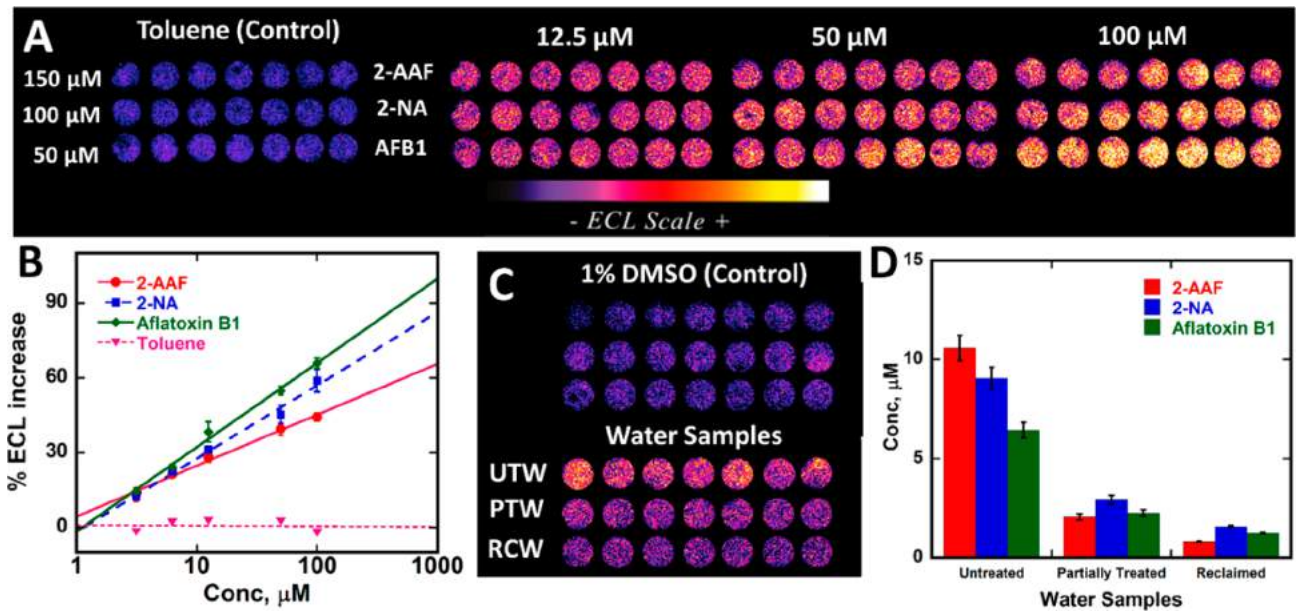

Figure 4. Array results for standards with known DNA-reactive metabolites: (A) Recolorized ECL data using arrays featuring RuPVP/enzyme/DNA microwells treated with oxygenated solutions of carcinogens (2-AAF, 2-NA, and aflatoxin B1 and negative control toluene in 1% DMSO + 10 mM phosphate buffer pH 7.4 for 45 s at −0.65 V vs Ag/AgCl, with ECL captured by CCD camera after subsequently applying 1.25 V vs Ag/AgCl for 180 s. (B) Calibration plots of %ECL increase over the blank vs concentration of standards. ECL intensity increases proportional to DNA damage. (C) ECL array results comparing ECL intensities obtained from untreated water (UTW), partially treated water (PTW), and fully treated reclaimed water (RCW) with respect to 1% DMSO controls. Recolorized ECL data from arrays with each row representing microwells containing RuPVP/enzyme/DNA layers treated with UTW, PTW, RCW, and 1% DMSO in buffer for 45 s at −0.65 V vs Ag/AgCL with ECL captured after subsequent application of 1.25 V vs Ag/AgCl for 180 s. (D) Bar graph showing chemical equivalents from %ECL response for different water samples.

DOI: 10.1021/acssensors.7b00118
ACS Sens. XXXX, XXX, XXX−XXX

water samples was ~10-fold larger than that for fully reclaimed water and ~2.4 fold larger than that for partially treated water..

DISCUSSION

The results above illustrate a novel, low cost, 3-D printed microfluidic array capable of assessing the genotoxic potential of environmental samples. The 3-D printed device with disposable microwell array containing enzyme/DNA/RuPVP films costs less than $1.00 to fabricate. Advantages of this device include multianalyte analysis, complete automation, on chip metabolite generation, and rapid detection of DNA damage (5 min). These disposable arrays are designed to "plug-in" to a reusable automation platform featuring microcontrollers, micropumps, and battery that costs $150. The array here was equipped with 21 detection microwells, but it is possible to expand to larger size to accommodate multiple enzymes, multiple analytes, and higher sample throughput.

DNA reactivity related to metabolites from smoke or vapor extracts measured by the array clearly suggests comparable genotoxic potential of tobacco and nicotine e-cigarettes when assayed by the same protocol (Figure 3). Expression of the signals in terms of levels of known tobacco chemicals with metabolites having high rates of DNA damage, e.g., NNK (Figure 3D) provides a reference point to assess the severity of possible genotoxicity, without having to determine individual DNA adducts by expensive LC-MS/MS assays. E-cigarette vapor was reported to have low concentrations of chemicals with potential to cause DNA damage[13] and could be assumed by some to be a safer alternative to tobacco cigarettes. However, our results suggest similar DNA damage from e-cigarette vapors and tobacco cigarette smoking.

Results also showed that genotoxic potential for non-nicotine e-cigarettes is about the same as that for filtered tobacco cigarettes, and 1.5−2-fold lower than that for e-cigarettes. DNA reactivity for 20 puffs of an e-cigarette was equivalent to about 83 μM NNK (1.6 μg/mL) (Figure 3C) compared to estimated levels of NNK in one tobacco cigarette of 46 μM (0.9 μg/mL). Unfiltered tobacco cigarettes gave DNA reactivity nearly 2 times greater than filtered tobacco cigarettes (Figure 3B and C). Even non-nicotine e-cigarettes showed significant DNA reactivity, similar to that of filtered tobacco cigarettes (Figure 3C).

The above results are consistent with recent reports using conventional assays that found significant DNA strand breaks, cytotoxic effects, and cell death caused by e-cigarette vapor with and without nicotine.[41,42] Ease of use of e-cigarettes may also result in elevated use compared to tobacco cigarettes, which can result in escalated DNA damage. For example, DNA reactivity as NNK equivalents in vapor extract from two full e-cigarette cartridges was 1.1 mM, roughly equivalent to 0.9 mM for 20 tobacco cigarettes (SI Table S1).

The arrays also revealed genotoxic potential of water samples (Figure 4). ECL responses from the untreated wastewater were about 9 times larger than those for fully recovered water, suggesting significant presence of genotoxic chemicals. Successful analysis of samples during midtreatment suggests that the array can be used to monitor the success of intermediate stages of water treatment. Expression of these results in terms of water polluting chemicals that cause metabolite-related DNA damage again provide a rapid assessment of relative severity of the contamination (Figure 4D). Calibration range and LOD of 3 μM for standard water pollutants (Figure 4B) suggests applications in rapid identification of seriously polluted water. Array results for the untreated water samples are consistent with reports of genotoxic chemicals in domestic and industrial wastewater.[43] ECL responses from fully reclaimed water did not show significant genotoxic potential when compared to controls, suggesting significant removal of genotoxic chemicals.

In summary, we described here a new, portable, low cost, automated, toxicity screening tool to detect metabolite-related genotoxicity chemistry from environmental samples. The 3-D printed array is fast and accurate in sensing effects of possible genotoxic chemicals. A unique feature is that test chemicals are converted to their metabolites so that metabolite reactivity toward genetic material can be measured rapidly and efficiently. This is a major attribute for assessment of possible genotoxic consequences of pollutant exposure from relevant samples.

ASSOCIATED CONTENT

Supporting Information

The Supporting Information is available free of charge on the ACS Publications website at DOI: 10.1021/acssensors.7b00118.

Sources of chemicals and reagents, 3-D print specifications, SEM images of PG sheets and microwells, schematic program upload and detailed instructions for PCB integration, artificial inhalation system for smoke/vapor extraction, reproducibility results, and table of genotoxic potential related standards (PDF)

AUTHOR INFORMATION

Corresponding Author

*E-mail: james.rusling@uconn.edu.

ORCID

James F. Rusling: 0000-0002-6117-3306

Author Contributions

The manuscript was written through contributions of all authors. All authors have given approval to the final version of the manuscript.

Notes

The authors declare no competing financial interest.

ACKNOWLEDGMENTS

The authors thank the National Institute of Environmental Health Sciences (NIEHS), NIH, Grant No. ES03154 for financial support. We thank Islam M. Mosa for SEM images.

REFERENCES

(1) (a) Caldwell, J. C. DEHP: Genotoxicity and potential carcinogenic mechanisms—A review. *Mutat. Res., Rev. Mutat. Res.* **2012**, *751*, 82−157. (b) Chen, R. J.; Chang, L. W.; Lin, P.; Wang, Y. J. Epigenetic effects and molecular mechanisms of tumorigenesis induced by cigarette smoke: an overview. *J. Oncol.* **2011**, *2011*, 654931.

(2) (a) Hvastkovs, E. G.; Schenkman, J. B.; Rusling, J. F. Metabolic toxicity screening using electrochemiluminescence arrays coupled with enzyme-DNA biocolloid reactors and liquid chromatography-mass spectrometry. *Annu. Rev. Anal. Chem.* **2012**, *5*, 79−105. (b) Hvastkovs, E. G.; Rusling, J. F. State-of-the-Art Metabolic Toxicity Screening and Pathway Evaluation. *Anal. Chem.* **2016**, *88*, 4584−4599.

(3) (a) Rogers, K. Recent advances in biosensor techniques for environmental monitoring. *Anal. Chim. Acta* **2006**, *568*, 222−231. (b) Long, F.; Zhu, A.; Shi, H. Recent advances in optical biosensors for environmental monitoring and early warning. *Sensors* **2013**, *13*, 13928−13948.

DOI: 10.1021/acssensors.7b00118
ACS Sens. XXXX, XXX, XXX−XXX

(4) Mani, V.; Kadimisetty, K.; Malla, S.; Joshi, A. A.; Rusling, J. F. Paper-based electrochemiluminescent screening for genotoxic activity in the environment. *Environ. Sci. Technol.* **2013**, *47*, 1937−1944.
(5) (a) Gross, B. C.; Erkal, J. L.; Lockwood, S. Y.; Chen, C.; Spence, D. M. Evaluation of 3D printing and its potential impact on biotechnology and the chemical sciences. *Anal. Chem.* **2014**, *86*, 3240−3253. (b) Bishop, G. W.; Satterwhite-Warden, J. E.; Kadimisetty, K.; Rusling, J. F. 3D-printed bioanalytical devices. *Nanotechnology* **2016**, *27*, 284002.
(6) (a) Lee, W.; Kwon, D.; Choi, W.; Jung, G. Y.; Au, A. K.; Folch, A.; Jeon, S. 3D-printed microfluidic device for the detection of pathogenic bacteria using size-based separation in helical channel with trapezoid cross-section. *Sci. Rep.* **2015**, *5*, 7717. (b) Coskun, A. F.; Nagi, R.; Sadeghi, K.; Phillips, S.; Ozcan, A. Albumin testing in urine using a smart-phone. *Lab Chip* **2013**, *13*, 4231−4238. (c) Wei, Q.; Luo, W.; Chiang, S.; Kappel, T.; Mejia, C.; Tseng, D.; Chan, R. Y. L.; Yan, E.; Qi, H.; Shabbir, F.; et al. Imaging and sizing of single DNA molecules on a mobile phone. *ACS Nano* **2014**, *8*, 12725−12733. (d) Coskun, A. F.; Wong, J.; Khodadadi, D.; Nagi, R.; Tey, A.; Ozcan, A. A personalized food allergen testing platform on a cellphone. *Lab Chip* **2013**, *13*, 636−640. (e) Wei, Q.; Nagi, R.; Sadeghi, K.; Feng, S.; Yan, E.; Ki, S. J.; Caire, R.; Tseng, D.; Ozcan, A. Detection and spatial mapping of mercury contamination in water samples using a smart-phone. *ACS Nano* **2014**, *8*, 1121−1129. (f) Kitson, P. J.; Rosnes, M. H.; Sans, V.; Dragone, V.; Cronin, L. Configurable 3D-Printed millifluidic and microfluidic 'lab on a chip'reactionware devices. *Lab Chip* **2012**, *12*, 3267−3271. (g) Kitson, P. J.; Symes, M. D.; Dragone, V.; Cronin, L. Combining 3D printing and liquid handling to produce user-friendly reactionware for chemical synthesis and purification. *Chemical Science* **2013**, *4*, 3099−3103. (h) Dragone, V.; Sans, V.; Rosnes, M. H.; Kitson, P. J.; Cronin, L. 3D-printed devices for continuous-flow organic chemistry. *Beilstein J. Org. Chem.* **2013**, *9*, 951−959.
(7) (a) Bhargava, K. C.; Thompson, B.; Malmstadt, N. Discrete elements for 3D microfluidics. *Proc. Natl. Acad. Sci. U. S. A.* **2014**, *111*, 15013−15018. (b) Snowden, M. E.; King, P. H.; Covington, J. A.; Macpherson, J. V.; Unwin, P. R. Fabrication of versatile channel flow cells for quantitative electroanalysis using prototyping. *Anal. Chem.* **2010**, *82*, 3124−3131. (c) Erkal, J. L.; Selimovic, A.; Gross, B. C.; Lockwood, S. Y.; Walton, E. L.; McNamara, S.; Martin, R. S.; Spence, D. M. 3D printed microfluidic devices with integrated versatile and reusable electrodes. *Lab Chip* **2014**, *14*, 2023−2032. (d) Saggiomo, V.; Velders, A. H. Simple 3D printed scaffold-removal method for the fabrication of intricate microfluidic devices. *Advanced Science* **2015**, *2*, 1500125. (e) Lee, K. G.; Park, K. J.; Seok, S.; Shin, S.; Park, J. Y.; Heo, Y. S.; Lee, S. J.; Lee, T. J. 3D printed modules for integrated microfluidic devices. *RSC Adv.* **2014**, *4*, 32876−32880.
(8) (a) Bishop, G. W.; Satterwhite, J. E.; Bhakta, S.; Kadimisetty, K.; Gillette, K. M.; Chen, E.; Rusling, J. F. 3D-printed fluidic devices for nanoparticle preparation and flow-injection amperometry using integrated prussian blue nanoparticle-modified electrodes. *Anal. Chem.* **2015**, *87*, 5437−5443. (b) Bishop, G. W.; Satterwhite-Warden, J. E.; Bist, I.; Chen, E.; Rusling, J. F. Electrochemiluminescence at bare and DNA-coated graphite electrodes in 3D-printed fluidic devices. *ACS Sens.* **2016**, *1*, 197−202.
(9) Kadimisetty, K.; Mosa, I. M.; Malla, S.; Satterwhite-Warden, J. E.; Kuhns, T. M.; Faria, R. C.; Lee, N. H.; Rusling, J. F. 3D-printed supercapacitor-powered electrochemiluminescent protein immunoarray. *Biosens. Bioelectron.* **2016**, *77*, 188−193.
(10) Thun, M. J.; Carter, B. D.; Feskanich, D.; Freedman, N. D.; Prentice, R.; Lopez, A. D.; Hartge, P.; Gapstur, S. M. 50-year trends in smoking-related mortality in the United States. *N. Engl. J. Med.* **2013**, *368*, 351−364. (b) Alexandrov, L. B.; Ju, Y. S.; Haase, K.; Van Loo, P.; Martincorena, I.; Nik-Zainal, S.; Totoki, Y.; Fujimoto, A.; Nakagawa, H.; Shibata, T.; et al. Mutational signatures associated with tobacco smoking in human cancer. *bioRxiv* **2016**, 051417.
(11) Mokdad, A. H.; Marks, J. S.; Stroup, D. F.; Gerberding, J. L. Actual causes of death in the United States, 2000. *JAMA* **2004**, *291*, 1238−1245.
(12) (a) Singh, T.; Arrazola, R. A.; Corey, C. G.; et al. Tobacco use among middle and high school students—United States, 2011−2015. *MMWR.Morbidity and mortality weekly report* **2016**, *65*, 361−367. (b) McMillen, R. C.; Gottlieb, M. A.; Shaefer, R. M.; Winickoff, J. P.; Klein, J. D. Trends in Electronic Cigarette Use Among U.S. Adults: Use is Increasing in Both Smokers and Nonsmokers. *Nicotine Tob. Res.* **2015**, *17*, 1195−1202.
(13) (a) Grana, R.; Benowitz, N.; Glantz, S. A. E-cigarettes: a scientific review. *Circulation* **2014**, *129*, 1972−1986. (b) Trtchounian, A.; Williams, M.; Talbot, P. Conventional and electronic cigarettes (e-cigarettes) have different smoking characteristics. *Nicotine Tob. Res.* **2010**, *12*, 905−912.
(14) Schwarzenbach, R. P.; Escher, B. I.; Fenner, K.; Hofstetter, T. B.; Johnson, C. A.; von Gunten, U.; Wehrli, B. The challenge of micropollutants in aquatic systems. *Science* **2006**, *313*, 1072−1077.
(15) Schwarzenbach, R. P.; Egli, T.; Hofstetter, T. B.; von Gunten, U.; Wehrli, B. Global water pollution and human health. *Annual Review of Environment and Resources* **2010**, *35*, 109−136.
(16) (a) Gruber, N.; Galloway, J. N. An Earth-system perspective of the global nitrogen cycle. *Nature* **2008**, *451*, 293−296. (b) Filippelli, G. M. The global phosphorus cycle: past, present, and future. *Elements* **2008**, *4*, 89−95. (c) Jorgenson, A. K. Political-economic Integration, Industrial Pollution and Human Health: A Panel Study of Less-Developed Countries, 1980—2000. *International Sociology* **2009**, *24*, 115−143. (d) Watson, S. B. Aquatic taste and odor: a primary signal of drinking-water integrity. *J. Toxicol. Environ. Health, Part A* **2004**, *67*, 1779−1795.
(17) Ohe, T.; Watanabe, T.; Wakabayashi, K. Mutagens in surface waters: a review. *Mutat. Res., Rev. Mutat. Res.* **2004**, *567*, 109−149.
(18) University of Connecticut (UCONN) water treatment facility; http://ecohusky.uconn.edu/water/rwf.html; last accessed 13 Feb 2017.
(19) Dennany, L.; Forster, R. J.; Rusling, J. F. Simultaneous direct electrochemiluminescence and catalytic voltammetry detection of DNA in ultrathin films. *J. Am. Chem. Soc.* **2003**, *125*, 5213−5218.
(20) http://web2.uconn.edu/rusling/3D_printing.html; last accessed 13 Feb 2017.
(21) Tang, C. K.; Vaze, A.; Rusling, J. F. Fabrication of immunosensor microwell arrays from gold compact discs for detection of cancer biomarker proteins. *Lab Chip* **2012**, *12*, 281−286.
(22) Rusling, J. F.; Wasalathanthri, D. P.; Schenkman, J. B. Thin multicomponent films for functional enzyme devices and bioreactor particles. *Soft Matter* **2014**, *10*, 8145−8156.
(23) http://www.atmel.com/devices/attiny85.aspx; last accessed 13 Feb 2017.
(24) Krishnan, S.; Hvastkovs, E. G.; Bajrami, B.; Choudhary, D.; Schenkman, J. B.; Rusling, J. F. Synergistic metabolic toxicity screening using microsome/DNA electrochemiluminescent arrays and nano-reactors. *Anal. Chem.* **2008**, *80*, 5279−5285.
(25) (a) Krishnan, S.; Wasalathanthri, D.; Zhao, L.; Schenkman, J. B.; Rusling, J. F. Efficient bioelectronic actuation of the natural catalytic pathway of human metabolic cytochrome P450s. *J. Am. Chem. Soc.* **2011**, *133*, 1459−1465. (b) Wasalathanthri, D. P.; Faria, R. C.; Malla, S.; Joshi, A. A.; Schenkman, J. B.; Rusling, J. F. Screening reactive metabolites bioactivated by multiple enzyme pathways using a multiplexed microfluidic system. *Analyst* **2013**, *138*, 171−178.
(26) (a) Etter, J.; Bullen, C. A longitudinal study of electronic cigarette users. *Addict. Behav.* **2014**, *39*, 491−494. (b) Etter, J.; Bullen, C. Electronic cigarette: users profile, utilization, satisfaction and perceived efficacy. *Addiction* **2011**, *106*, 2017−2028. (c) Etter, J. Electronic cigarettes: a survey of users. *BMC Public Health* **2010**, *10*, 231.
(27) Shihadeh, A.; Saleh, R. Polycyclic aromatic hydrocarbons, carbon monoxide,"tar", and nicotine in the mainstream smoke aerosol of the narghile water pipe. *Food Chem. Toxicol.* **2005**, *43*, 655−661.
(28) (a) Grana, R. A.; Ling, P. M. Smoking revolution": a content analysis of electronic cigarette retail websites. *Am. J. Prev. Med.* **2014**, *46*, 395−403. (b) Goniewicz, M. L.; Kuma, T.; Gawron, M.; Knysak,

DOI: 10.1021/acssensors.7b00118
ACS Sens. XXXX, XXX, XXX−XXX

J.; Kosmider, L. Nicotine levels in electronic cigarettes. *Nicotine Tob. Res.* **2013**, *15*, 158−166.
(29) López-Barea, J.; Pueyo, C. Mutagen content and metabolic activation of promutagens by molluscs as biomarkers of marine pollution. *Mutat. Res., Fundam. Mol. Mech. Mutagen.* **1998**, *399*, 3−15.
(30) Le Curieux, F.; Marzin, D.; Erb, F. Comparison of three short-term assays: results on seven chemicals: Potential contribution to the control of water genotoxicity. *Mutat. Res., Genet. Toxicol. Test.* **1993**, *319*, 223−236.
(31) Žegura, B.; Heath, E.; Černoša, A.; Filipič, M. Combination of in vitro bioassays for the determination of cytotoxic and genotoxic potential of wastewater, surface water and drinking water samples. *Chemosphere* **2009**, *75*, 1453−1460.
(32) Pan, S.; Zhao, L.; Schenkman, J. B.; Rusling, J. F. Evaluation of electrochemiluminescent metabolic toxicity screening arrays using a multiple compound set. *Anal. Chem.* **2011**, *83*, 2754−2760.
(33) (a) Xue, W.; Warshawsky, D. Metabolic activation of polycyclic and heterocyclic aromatic hydrocarbons and DNA damage: a review. *Toxicol. Appl. Pharmacol.* **2005**, *206*, 73−93. (b) Straif, K.; Baan, R.; Grosse, Y.; Secretan, B.; El Ghissassi, F.; Cogliano, V. Carcinogenicity of polycyclic aromatic hydrocarbons. *Lancet Oncol.* **2005**, *6*, 931.
(34) Hecht, S. S. Tobacco carcinogens, their biomarkers and tobacco-induced cancer. *Nat. Rev. Cancer* **2003**, *3*, 733−744.
(35) Wasalathanthri, D. P.; Li, D.; Song, D.; Zheng, Z.; Choudhary, D.; Jansson, I.; Lu, X.; Schenkman, J. B.; Rusling, J. F. Elucidating organ-specific metabolic toxicity chemistry from electrochemiluminescent enzyme/DNA arrays and bioreactor bead-LC-MS/MS. *Chemical Science* **2015**, *6*, 2457−2468.
(36) Warth, B.; Sulyok, M.; Krska, R. LC-MS/MS-based multibiomarker approaches for the assessment of human exposure to mycotoxins. *Anal. Bioanal. Chem.* **2013**, *405*, 5687−5695.
(37) Phillips, D. H.; Farmer, P. B.; Beland, F. A.; Nath, R. G.; Poirier, M. C.; Reddy, M. V.; Turteltaub, K. W. Methods of DNA adduct determination and their application to testing compounds for genotoxicity. *Environ. Mol. Mutagen.* **2000**, *35*, 222−233.
(38) Yu, M. Y.; Skipper, P. L.; Tannenbaum, S. R.; Chan, K. K.; Ross, R. K. Arylamine exposures and bladder cancer risk. *Mutat. Res., Fundam. Mol. Mech. Mutagen.* **2002**, *506*, 21−28.
(39) Wasalathanthri, D. P.; Faria, R. C.; Malla, S.; Joshi, A. A.; Schenkman, J. B.; Rusling, J. F. Screening reactive metabolites bioactivated by multiple enzyme pathways using a multiplexed microfluidic system. *Analyst* **2013**, *138*, 171−178.
(40) Arlt, V. M.; Schmeiser, H. H.; Osborne, M. R.; Kawanishi, M.; Kanno, T.; Yagi, T.; Phillips, D. H.; Takamura-Enya, T. Identification of three major DNA adducts formed by the carcinogenic air pollutant 3-nitrobenzanthrone in rat lung at the C8 and N2 position of guanine and at the N6 position of adenine. *Int. J. Cancer* **2006**, *118*, 2139−2146.
(41) Yu, V.; Rahimy, M.; Korrapati, A.; Xuan, Y.; Zou, A. E.; Krishnan, A. R.; Tsui, T.; Aguilera, J. A.; Advani, S.; Alexander, L. E. C.; et al. Electronic cigarettes induce DNA strand breaks and cell death independently of nicotine in cell lines. *Oral Oncol.* **2016**, *52*, 58−65.
(42) (a) Wei, B.; Blount, B. C.; Xia, B.; Wang, L. Assessing exposure to tobacco-specific carcinogen NNK using its urinary metabolite NNAL measured in US population: 2011−2012. *J. Exposure Sci. Environ. Epidemiol.* **2016**, *26*, 249−256. (b) Zhong, Y.; Carmella, S. G.; Upadhyaya, P.; Hochalter, J. B.; Rauch, D.; Oliver, A.; Jensen, J.; Hatsukami, D.; Wang, J.; Zimmerman, C.; Hecht, S. S. Immediate consequences of cigarette smoking: rapid formation of polycyclic aromatic hydrocarbon diol epoxides. *Chem. Res. Toxicol.* **2011**, *24*, 246−252.
(43) (a) White, P. A.; Rasmussen, J. B. The genotoxic hazards of domestic wastes in surface waters. *Mutat. Res., Rev. Mutat. Res.* **1998**, *410*, 223−236. (b) Thewes, M. R.; Endres Junior, D.; Droste, A. Genotoxicity biomonitoring of sewage in two municipal wastewater treatment plants using the Tradescantia pallida var. purpurea bioassay. *Genet. Mol. Biol.* **2011**, *34*, 689−693. (c) Žegura, B.; Heath, E.; Černoša, A.; Filipič, M. Combination of in vitro bioassays for the determination of cytotoxic and genotoxic potential of wastewater, surface water and drinking water samples. *Chemosphere* **2009**, *75*, 1453−1460.

DOI: 10.1021/acssensors.7b00118
ACS Sens. XXXX, XXX, XXX−XXX